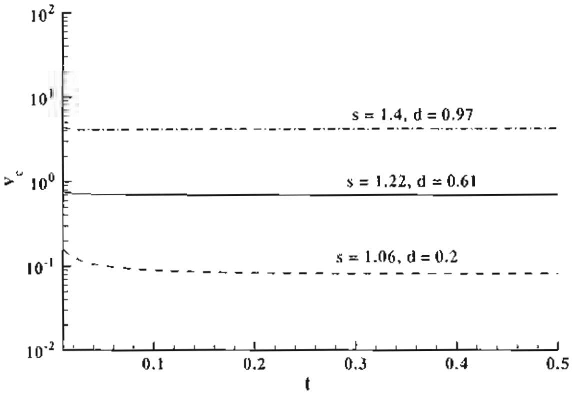

Figure 13. Variations with time of variance at the lower left corner (v_c) of MFSHE solutions to the third test problem.

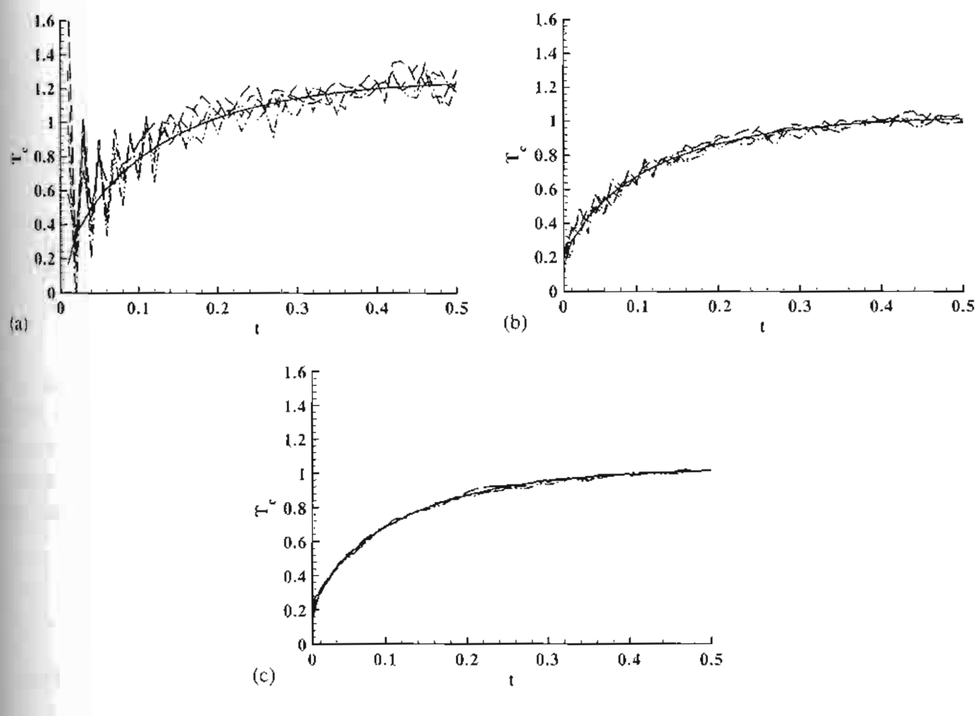

Figure 14. Variations with time of temperature at the lower left corner (T_c) from MFSMH solutions to the problem without exact solution. The solid line represents the solution corresponding to exact initial and boundary conditions, whereas four other lines represent solutions corresponding to four sets of random initial and boundary conditions: (a) $s = 1.3$, $c = 0.6$; (b) $s = 1.2$, $c = 0.4$; and (c) $s = 1.1$, $c = 0.2$.

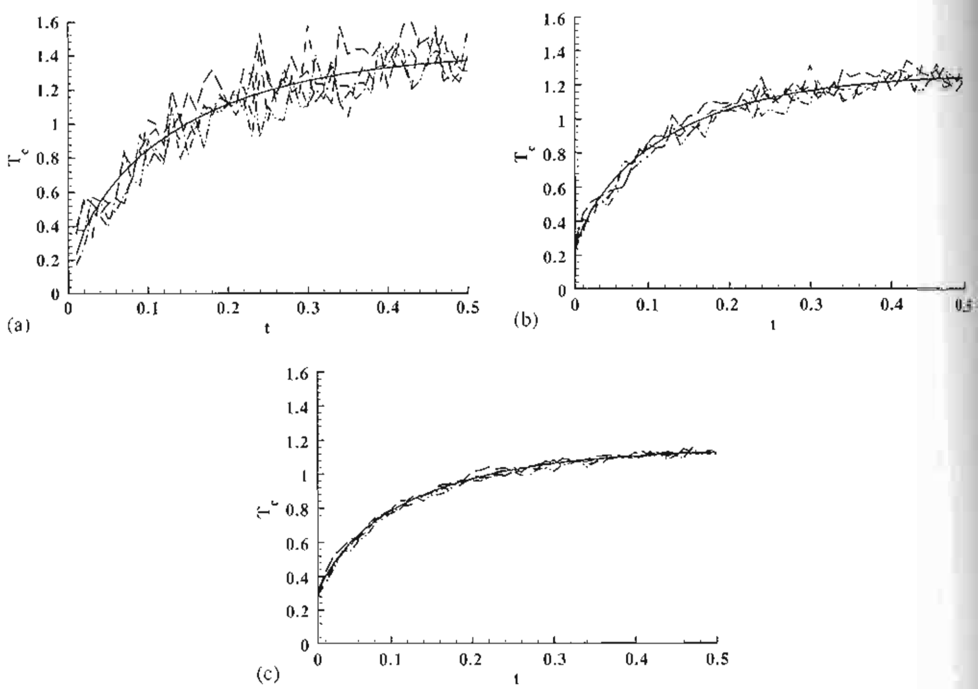

Figure 15. Variations with time of temperature at the lower left corner (T_c) from MFSHE solutions to the problem without exact solution. The solid line represents the solution corresponding to exact initial and boundary conditions, whereas four other lines represent solutions corresponding to four sets of random initial and boundary conditions: (a) $s = 1.4$, $d = 0.97$; (b) $s = 1.22$, $d = 0.61$; and (c) $s = 1.06$, $d = 0.2$.

to evaluate performances of MFSMH and MFSHE, the expression of the solution of ea method in terms of the initial and boundary conditions is derived. It is found that MFSM performs better than MFSHE in solving three test problems having different boundary conditio because MFSMH solutions are more accurate and less sensitive to uncertainties in initial a boundary conditions than MFSHE solutions. Furthermore, MFSMH produces solutions that comparable to FDM solutions.

ACKNOWLEDGEMENTS

The author would like to acknowledge the financial support from the Thailand Research Fund.

REFERENCES

1. Karageorghis A, Fairweather G. The method of fundamental solutions for the numerical solution of biharmonic equation. *Journal of Computational Physics* 1987; **69**(2):434–459.
2. Golberg MA. The method of fundamental solutions for Poisson's equations. *Engineering Analysis* *Boundary Elements* 1995; **16**(3):205–213.

3. Poullikkas A, Karageorghis A, Georgiou G. The method of fundamental solutions for inhomogeneous elliptic problems. *Computational Mechanics* 1998; **22**(1):100–107.
4. Balakrishnan K, Ramachandran PA. The method of fundamental solutions for linear diffusion–reaction equations. *Mathematical and Computer Modelling* 2000; **31**(2–3):221–237.
5. Chantasiriwan S. Cartesian grid methods using radial basis functions for solving Poisson, Helmholtz, and diffusion convection equations. *Engineering Analysis with Boundary Elements* 2004; **28**(12):1417–1425.
6. Partridge PW, Sensale B. The method of fundamental solutions with dual reciprocity for diffusion and diffusion-convection using subdomains. *Engineering Analysis with Boundary Elements* 2000; **24**(9):633–641.
7. Balakrishnan K, Sureshkumar R, Ramachandran PA. An operator splitting-radial basis function method for the solution of transient nonlinear Poisson problems. *Computers and Mathematics with Applications* 2000; **43**(3–5):289–304.
8. Li J, Hon YC, Chen CS. Numerical comparisons of two meshless methods using radial basis functions. *Engineering Analysis with Boundary Elements* 2000; **26**(3):205–225.
9. Young DL, Tsai CC, Murugesan K, Fan CW, Chen CW. Time-dependent fundamental solutions for homogeneous diffusion problems. *Engineering Analysis with Boundary Elements* 2004; **28**(12):1463–1473.
10. Kansa EJ. Multiquadrics—A scattered data approximation scheme with applications to computational fluid-dynamics II solutions to parabolic, hyperbolic and elliptic partial differential equations. *Computers and Mathematics with Applications* 1990; **19**(8–9):147–161.

ELSEVIER

Available online at www.sciencedirect.com
SCIENCE DIRECT

International Communications in Heat and Mass Transfer 33 (2006) 342 – 349

International Communications in HEAT and MASS TRANSFER

www.elsevier.com/locate/ichmt

Error and variance of solution to the stochastic heat conduction problem by multiquadric collocation method ☆

Somchart Chantasiriwan

Faculty of Engineering, Thammasat University, Pathum Thani 12121, Thailand

Available online 29 November 2005

Abstract

Error and variance of the solution to the heat conduction problem having stochastic initial and boundary conditions are determined by a formulation based on a meshless method known as the multiquadric collocation method. This formulation expresses the solution in terms of initial and boundary conditions. Inspection of solutions to two test problems reveals that a large value of the shape parameter, which is the free parameter of multiquadrics, should not be used for a stochastic problem because it may lead to a solution that is too sensitive to uncertainties in boundary and initial conditions.

Keywords: Stochastic; Meshless; Radial basis function

1. Introduction

A radial basis function is a function that depends on the distance between the point where the function is to be evaluated and the center point. Radial basis functions have been used for multivariate data interpolation. Multiquadrics is a well-known radial basis function that has been shown to converge faster than other radial basis functions [1]. Kansa extended the use of multiquadrics in a collocation method for solving partial differential equations [2]. The multiquadric collocation method or the Kansa's method has been successfully used to solve steady-state problems [3–5] and time-dependent problems [6–8]. Compared with conventional methods such as the finite element method and the finite difference method, the multiquadric collocation method has advantages that include easy implementation, simple preprocessing, and ability to handle complex geometries. A system of algebraic equations produced by the multiquadric collocation method has a dense coefficient matrix, which is considered to be a disadvantage. However, the prospect of cheaper computers with higher computing power may lessen the importance of this disadvantage. The free parameter in multiquadrics, known as the shape parameter, affects solution accuracy. Cheng et al. [9] showed that the accuracy of the solution to a partial differential equation can be increased either by decreasing the mesh size or increasing the shape parameter. The latter method seems like an efficient way to achieve high accuracy. However, the shape of multiquadrics becomes increasingly flat as the shape parameter is increased, giving rise to ill-conditioned coefficient matrix. When the shape parameter is too large, round-off error dominates, and the solution loses its accuracy. Therefore, in order to obtain a very accurate solution by the multiquadric collocation method, a machine with higher computing power is needed so that computation can be performed with higher

☆ Communicated by W.J. Minkowycz.
E-mail address: somchart@engr.tu.ac.th.

doi:10.1016/j.icheatmasstransfer.2005.10.014

Nomenclature

$a_j^{(n)}$	Coefficient
B	Boundary value operator
$\mathbf{B}$, $\mathbf{C}$	Coefficient matrices
c	The shape parameter of multiquadrics
$\mathbf{D}_1$, $\mathbf{D}_2$	Coefficient matrices
e	Average error
f	Probability density function for random error
g	Boundary value
N	The total number of nodes
N_b	The number of boundary nodes
N_i	The number of interior nodes
n	Time level
T	Temperature
T_0	Initial temperature
t	Time coordinate
Δt	Time step
v	Normalized average variance
X	Coefficient of the relation between the solution and the initial condition
Y	Coefficient of the relation between the solution and the boundary condition
x, y	Space coordinates
ε_1, ε_2	Random error
$\mathbf{\Phi}$	Coefficient matrix
ϕ	Multiquadrics
σ^2	Variance of random errors in initial and boundary conditions

precision. Alternatively, the Contour–Pade algorithm, proposed by Fornberg and Wright [10], may be used. T algorithm enables stable computation of multiquadric interpolation for large values of the shape parameter using o a desktop computer. Larsson and Fornberg [11] applied this algorithm in solving elliptic partial differential equatio

It is well known that actual engineering problems such as heat conduction problems are characterized uncertainties in material properties, boundary, and initial conditions. Unfortunately, most previous applications of multiquadric collocation method have not paid attention to sensitivities of solutions to these uncertainties. Since v few actual heat conduction problems are deterministic problems, the quality of the solution to such a problem sho depend not only on the accuracy but also the variance of the solution. In this paper, the formulation of the multiqua collocation method for solving time-dependent heat conduction problem having stochastic boundary and ini conditions is considered. In order to determine accuracy and variance, the solution will be expressed in terms boundary and initial conditions. Two test problems will be used to assess the performance of the multiquad collocation method.

2. Multiquadric collocation method

Consider a non-dimensional deterministic problem described by the following governing equation, initial boundary conditions.

$$\frac{\partial T}{\partial t} = \frac{\partial^2 T}{\partial x^2} + \frac{\partial^2 T}{\partial y^2}$$

$$B\{T(x,y,t)\} = g(x,y,t)$$

$$T(x,y,0) = T_0(x,y)$$

here $B=1$ for Dirichlet boundary and $\partial/\partial n$ for Neumann boundary, with n being the coordinate normal to the undary. Discretization of Eq. (1) yields

$$\frac{T^{(n)}-T^{(n-1)}}{\Delta t} = 0.5\nabla^2 T^{(n)} + 0.5\nabla^2 T^{(n-1)} \tag{4}$$

hich can be rearranged into an inhomogeneous modified Helmholtz equation.

$$\nabla^2 T^{(n)} - \frac{2T^{(n)}}{\Delta t} = -\nabla^2 T^{(n-1)} - \frac{2T^{(n-1)}}{\Delta t}. \tag{5}$$

Assume that there are N nodes, divided into N_i interior nodes and N_b boundary nodes. Let $\vec{r}_i$ ($i=1, 2, \ldots, N_\mathrm{i}$) denote ositions of interior nodes, and $\vec{r}_i$ ($i=N_\mathrm{i}+1, N_\mathrm{i}+2, \ldots, N_\mathrm{i}+N_\mathrm{b}$) denote positions of boundary nodes. The multiquadric llocation method approximates T as follows.

$$T(x,y,n\Delta t) = \sum_{j=1}^{N} a_j^{(n)} \phi(x,y,x_j,y_j) \tag{6}$$

here

$$\phi(x,y,x_j,y_j) = \sqrt{(x-x_j)^2 + (y-y_j)^2 + c^2} \tag{7}$$

s known as multiquadrics. Note that this function contains the shape parameter c. This parameter may either be a onstant or a variable. For simple implementation, c is chosen to be a constant in this paper. Eq. (6) leads to the ollowing matrix equation.

$$\vec{T}^{(n)} = \Phi \vec{a}^{(n)} \tag{8}$$

here $\vec{T}^{(n)}$ is the vector of nodal temperatures at time $n\Delta t$, and $\vec{a}^{(n)}$ is the vector of coefficients at time $n\Delta t$. Inserting Eq. (6) into Eqs. (2), (3) and (5) results in

$$\begin{aligned} &\sum_{j=1}^{N} a_j^{(n)} \nabla_i^2 \phi(x_i,y_i,x_j,y_j) - \frac{2}{\Delta t}\sum_{j=1}^{N} a_j^{(n)} \phi(x_i,y_i,x_j,y_j) \\ &\quad = -\sum_{j=1}^{N} a_j^{(n-1)} \nabla_i^2 \phi(x_i,y_i,x_j,y_j) - \frac{2}{\Delta t}\sum_{j=1}^{N} a_j^{(n-1)} \phi(x_i,y_i,x_j,y_j) \qquad (i = 1,2,\ldots N_\mathrm{i}) \end{aligned} \tag{9}$$

$$\sum_{j=1}^{N} a_j^{(n)} B\{\phi(x_i,y_i,x_j,y_j) = g(x_i,y_i,n\Delta t) \qquad (i = N_\mathrm{i}+1, N_\mathrm{i}+2, \ldots, N) \tag{10}$$

$$\sum_{j=1}^{N} a_j^{(0)} \phi(x_i,y_i,x_j,y_j) = T_0(x_i,y_i,0) \qquad (i = 1,2,\ldots N) \tag{11}$$

Eqs. (9) and (10) may be rewritten as a matrix equation:

$$\mathbf{B}\vec{a}^{(n)} = \mathbf{C}\begin{bmatrix} \vec{a}^{(n-1)} \\ \vec{g}^{(n)} \end{bmatrix} \tag{12}$$

hich can be solved to obtain a recurrence formula for $\vec{a}^{(n)}$

$$\vec{a}^{(n)} = \mathbf{D}_1 \vec{a}^{(n-1)} + \mathbf{D}_2 \vec{g}^{(n)} \tag{13}$$

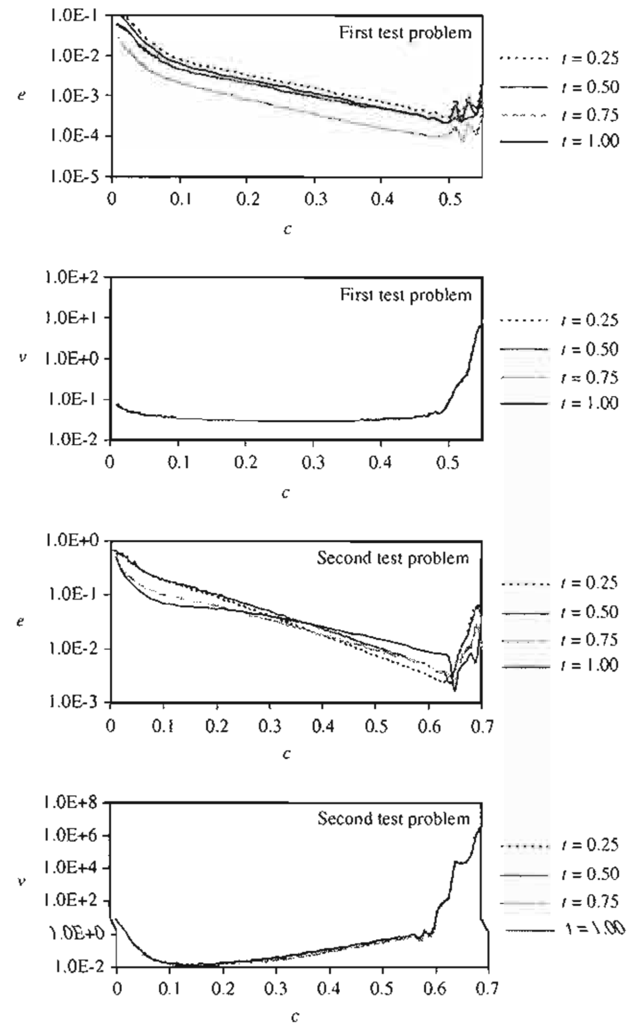

Fig. 1. Variations with the shape parameter of errors and variances of solutions to the two test problems corresponding to $N=121$ and $\Delta t=$ four times.

Eq. (11) may be rewritten as

$$\Phi \vec{a}^{(0)} = \vec{T}_0 \tag{14}$$

which can be solved for $\vec{a}^{(0)}$.

$$\vec{a}^{(0)} = \Phi^{-1} T_0 \tag{15}$$

Combining Eqs. (8), (13) and (15) gives an expression for the solution in terms of initial and boundary conditions

$$\vec{T}^{(n)} = \Phi \mathbf{D}_1^n \Phi^{-1} \vec{T}_0 + \Phi \sum_{k=1}^{n} \mathbf{D}_1^{n-i} \mathbf{D}_2 \vec{g}^{(k)} \tag{16}$$

or

$$T_i^{(n)} = \sum_{j=1}^{N} (X_{i,j})(T_0)_j + \sum_{k=1}^{n} \sum_{j=1}^{N_b} \left(Y_{i,j}^k\right) g_{N_i+j}^{(k)}. \tag{17}$$

Stochastic heat conduction problem

In stochastic heat conduction problems under consideration, material properties are deterministic, whereas boundary d initial conditions are stochastic. Therefore, these problems are described by Eq. (1), and the proposed multiquadric llocation method is applicable. Let $\bar{T}_0(x_i,y_i)$ and $\bar{g}(x_i,y_i,n\Delta t)$ be expected values of initial and boundary conditions at le i and time $n\Delta t$. Random functions of initial and boundary conditions are given by

$$T_0(x_i,y_i) = \bar{T}_0(x_i,y_i) + \varepsilon_1(x_i,y_i) \tag{18}$$

$$g(x_i,y_i,n\Delta t) = \bar{g}(x_i,y_i,n\Delta t) + \varepsilon_2(x_i,y_i,n\Delta t) \tag{19}$$

ere ε_1 and ε_2 are random errors. Assume that the probability density function for ε_1 and ε_2 is

$$f(\varepsilon) = \frac{1}{\sigma\sqrt{2\pi}}\exp\left[-\frac{1}{2}\left(\frac{\varepsilon}{\sigma}\right)^2\right] \tag{20}$$

hat the expected value of ε_1 and ε_2 is zero, and the variance of ε_1 and ε_2 is σ^2. Moreover, random errors at different les or times are uncorrelated. As a result, the expected value and variance of the solution at node i are

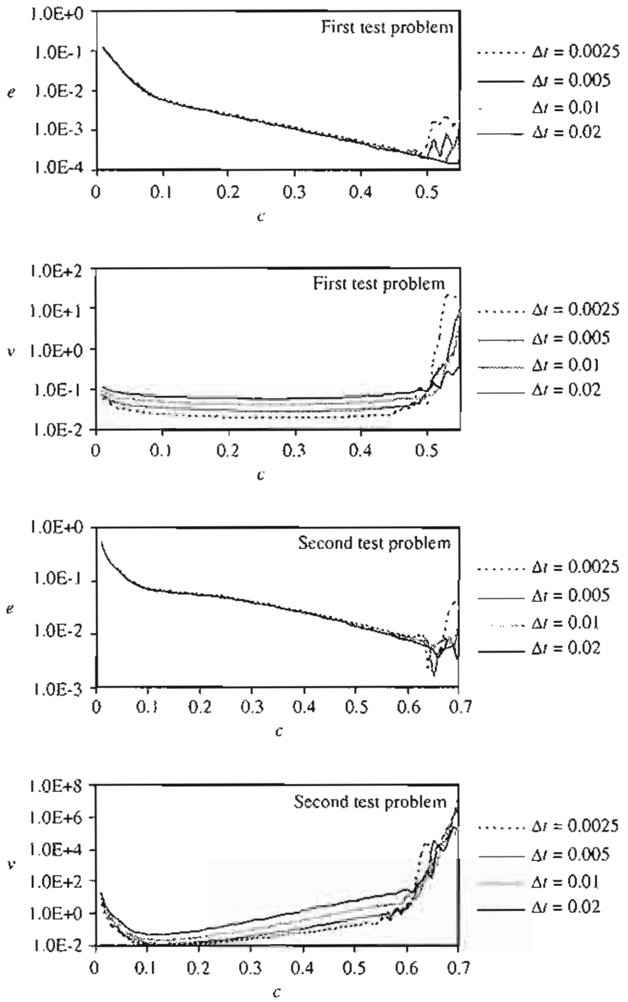

2. Variations with the shape parameter of errors and variances of solutions to the two test problems corresponding to $N = 121$ and four time steps at 00.

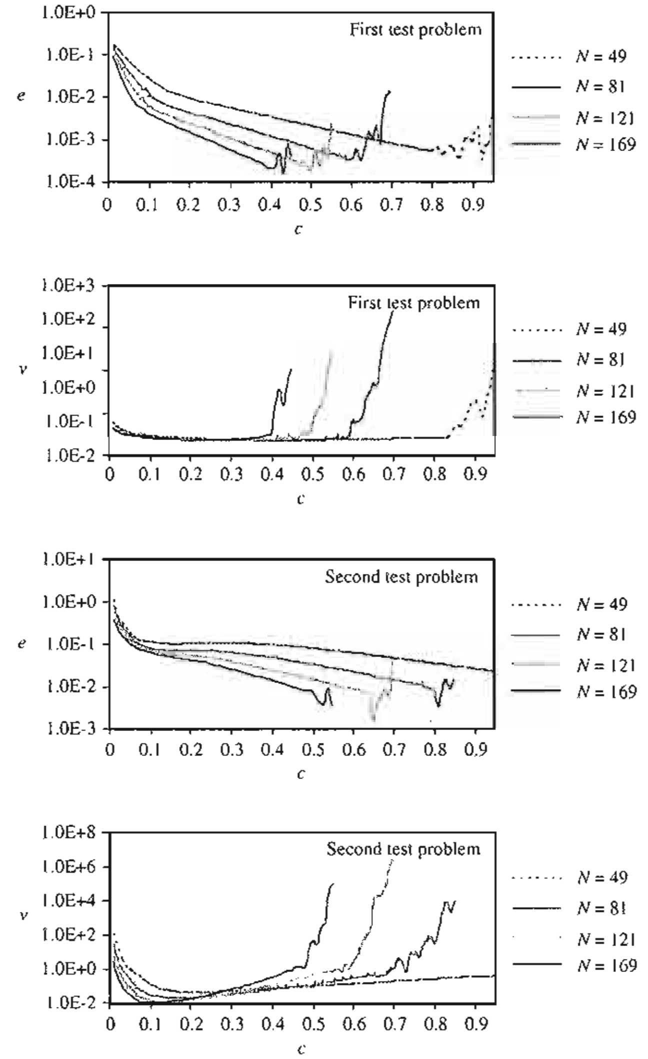

Fig. 3. Variations with the shape parameter of errors and variances of solutions to the two test problems corresponding to four numbers of nodes $\Delta t = 0.005$ at $t = 1.00$.

$$E\left(T_i^{(n)}\right) = \sum_{j=1}^{N} (X_{i,j})(\bar{T}_0)_j + \sum_{k=1}^{n} \sum_{j=1}^{N_b} \left(Y_{i,j}^{(k)}\right) \bar{g}_{N_{i+j}}^{(k)}$$

$$\mathrm{Var}\left(T_i^{(n)}\right) = \left[\sum_{j=1}^{N} (X_{i,j})^2 + \sum_{k=1}^{n} \sum_{j=1}^{N_b} \left(Y_{i,j}^{(k)}\right)^2\right] \sigma^2$$

If the exact solution in case of no random errors is available, the average error may be computed from

$$e = \sqrt{\frac{\sum_{i=1}^{N_i} \left[E\left(T_i^{(n)}\right) - \left(T_i^{(n)}\right)_{\mathrm{exact}}\right]^2}{\sum_{i=1}^{N_i} \left(T_i^{(n)}\right)^2_{\mathrm{exact}}}}$$

and the normalized average variance may be computed from

$$v = \frac{1}{N_i\sigma^2}\sum_{i=1}^{N_i}\mathrm{Var}\left(T_i^{(n)}\right) \tag{24}$$

4. Results and discussion

Consider two test problems in a 1 × 1 square domain. In the first test problem, all four sides of the domain are subjected to the Dirichlet boundary condition. In the second test problem, all four sides of the domain are subjected to the Neumann boundary condition. The exact solution for both problems is

$$T_{\mathrm{exact}}(x,y,t) = e^{(x+y)}\cos(x+y+4t) \tag{25}$$

This solution is used to generate $g(x,y,t)$ and $T_0(x,y)$. The multiquadric collocation method is then used to calculate the solution at each interior node, from which e and v are determined using Eqs. (23) and (24). Several parameters affect the solution. Considered parameters are the shape parameter, time step, time, the number of nodes, and grid spacing. Let there be N nodes distributed uniformly in the domain so that $N_i = (\sqrt{N}-2)^2$, $N_b = 4(\sqrt{N}-1)$, and the grid spacing is $\Delta = 1/(\sqrt{N}-1)$. Results obtained for the two test problems are shown in Figs. 1–3.

Variations of average errors and normalized average variances at t=0.25, 0.50, 0.75, and 1.00 with the shape parameter for the two test problems are shown in Fig. 1. In this figure, the number of nodes and the time step are kept constant at 121 and 0.005, respectively. Errors decrease monotonically with the shape parameter until solutions become unstable due to large condition numbers. Variances initially decrease with increasing shape parameter, reach minimum values, and then increase rapidly. Therefore, although solutions are quite accurate at a large value of the shape parameter, they are also very sensitive to random errors in initial and boundary conditions.

Variations of average errors and normalized average variances at t= 1.00 with the shape parameter corresponding to time steps of 0.0025, 0.005, 0.01, and 0.02 for the two test problems are shown in Fig. 2. In this figure, the number of nodes is kept constant at 121. Effects of the shape parameters on variations of errors and variances in Fig. 2 are similar to those in Figs. 1 and 2. In addition, it is interesting to note that a smaller time step leads to a solution of lower variance without affecting the accuracy of the solution significantly.

Variations of average errors and normalized average variances at t= 1.00 with shape parameter corresponding to numbers of nodes of 49, 81, 121, and 169 for the two test problems are shown in Fig. 3. In this figure, the time step is kept constant at 0.005. Again, effects of shape parameters on variations of errors and variances in Fig. 3 are similar to those in Fig. 1. In addition, it is interesting to note that the larger number of nodes leads to instability at a smaller value of shape parameter.

5. Conclusions

Formulation of the multiquadric collocation method for solving the heat equation having stochastic initial and boundary conditions is presented. The solution is expressed in terms of initial and boundary conditions, enabling straightforward computation of error and variance. Two test problems are used to show effects on various parameters on errors and variances of solutions. It is found that, with the same parameters, the solution to the test problem that has only the Dirichlet boundary condition and the solution to the test problem that has only the Neumann boundary condition behave similarly. It is also found that the parameter that affects solutions most significantly is the shape parameter of multiquadrics. Solutions become more accurate as the shape parameter increases. However, when the shape parameter is too large, solutions become unstable and very sensitive to random errors in initial and boundary conditions. Similar results were obtained by Chantasiriwan in solving steady-state problems with stochastic boundary conditions by the multiquadric collocation method [12].

Acknowledgments

This research has been financially supported by the Thailand Research Fund.

References

[1] R. Franke, Scattered data interpolation: tests of some methods, Mathematics of Computation 38 (1982) 181–200.

[2] E.J. Kansa, Multiquadrics—a scattered data approximation scheme with applications to computational fluid dynamics: II, Computer and Mathematics with Applications 19 (8–9) (1990) 147–161.

[3] X. Zhang, K.Z. Song, M.W. Lu, X. Liu, Meshless methods based on collocation with radial basis functions, Computational Mechanics (2000) 333–343.

[4] A.J.M. Ferreira, A formulation of the multiquadric radial basis function method for the analysis of laminated composite plates, Comp Structures 59 (3) (2003) 385–392.

[5] S. Chantasiriwan, Cartesian grid methods using radial basis functions for solving Poisson, Helmholtz, and diffusion–convection eq Engineering Analysis with Boundary Elements 28 (12) (2004) 1417–1425.

[6] M. Zerroukat, H. Power, C.S. Chen, A numerical method for heat transfer problems using collocation and radial basis functions, Intern Journal for Numerical Methods in Engineering 42 (7) (1998) 1263–1278.

[7] A.J.M. Ferreira, P.A.L.S. Martins, C.M.C. Roque, Solving time-dependent engineering problems with multiquadrics, Journal of Sou Vibration 280 (3–5) (2005) 595–610.

[8] S.A. Sarra, Adaptive radial basis function methods for time dependent partial differential equations, Applied Numerical Mathematics (2005) 79–94.

[9] A.H.-D. Cheng, M.A. Golberg, E.J. Kansa, Q. Zammito, Exponential convergence and H-c multiquadric collocation method for differential equations, Numerical Methods for Partial Differential Equations 19 (5) (2003) 571–594.

[10] B. Fornberg, G. Wright, Stable computation of multiquadric interpolants for all values of the shape parameter, Computer and Mathemati Applications 48 (5–6) (2004) 853–867.

[11] E. Larsson, B. Fornberg, A numerical study of some radial basis function based solution methods for elliptic PDEs, Computer and Math with Applications 46 (5–6) (2003) 891–902.

[12] S. Chantasiriwan, Solutions of partial differential equations with random Dirichlet boundary conditions by multiquadric collocation Engineering Analysis with Boundary Elements 29 (12) (2005) 1124–1129.

CNM 888 pp: 1–10 (col.fig.: Nil) PROD. TYPE: COM ED: Abraham PAGN: Vidya -- SCAN: nil

COMMUNICATIONS IN NUMERICAL METHODS IN ENGINEERING
Commun. Numer. Meth. Engng (in press)
Published online in Wiley InterScience (www.interscience.wiley.com). DOI: 10.1002/cnm.888

Collocation methods based on radial basis functions for solving stochastic Poisson problems

Somchart Chantasiriwan*,†

Faculty of Engineering, Thammasat University, Rangsit Campus, Pathum Thani 12121, Thailand

SUMMARY

Collocation methods based on radial basis functions can be used to provide accurate solutions to deterministic problems. For stochastic problems, accurate solutions may not be desirable if they are too sensitive to random inputs. In this paper, four methods are used to solve stochastic Poisson problems by expressing solutions in terms of source terms and boundary conditions. Comparison among the methods reveals that the method based on fundamental solutions performs better than other methods.

Received 11 August 2005; Revised 25 December 2005; Accepted 8 May 2006

KEY WORDS: multiquadrics; Hermite collocation; method of fundamental solutions

1. INTRODUCTION

It is customary to judge the performance of a numerical method by its accuracy. However, if inputs to the problem are stochastic, the solution will also be stochastic. Two important statistical properties of the solution are its expected value and its variance. In this case, the performance of the numerical method should be judged by both the accuracy and the variance of its solution because an accurate solution would be useful only if inputs are known exactly. In reality, there are always uncertainties in inputs, which will cause a solution of high accuracy and large variance to be useless in practice.

A Poisson problem is stochastic when the source term or the boundary condition is stochastic. Conventional methods such as the finite difference method and the finite element method can be shown to produce a solution that is insensitive to randomness in the source term or the boundary condition. Recently, collocation methods based on radial basis functions have gained interest from

*Correspondence to: Somchart Chantasiriwan, Faculty of Engineering, Thammasat University, Rangsit Campus, Pathum Thani 12121, Thailand.
†E-mail: somchart@engr.tu.ac.th

Contract/grant sponsor: The Thailand Research Fund; contract/grant number: RSA4680018

researchers due to the ability of these methods to solve various types of problems accurately. Whereas conventional methods produce sparse coefficient matrices with small condition numbers, these collocation methods produce dense coefficient matrices with large condition numbers. Therefore, it is unreasonable to assume that these methods behave similar to conventional methods in solving stochastic problems. It is important that collocation methods based on radial basis functions must be shown to produce solutions of satisfactory accuracy and variance before they can be used with confidence.

This paper describes formulations of four collocation methods for solving stochastic Poisson problems. Three methods use multiquadrics for collocation at both interior nodes and boundary nodes, whereas the fourth method uses multiquadrics for collocation at interior nodes and fundamental solutions for collocation at boundary nodes. Solutions are expressed in terms of source terms and boundary conditions so that errors and variances are computed conveniently. Influences of free parameters of the methods on the solutions are investigated, and the performances of the four methods in solving two test problems are compared.

2. COLLOCATION METHODS

Consider the following Poisson problem:

$$\frac{\partial^2 u}{\partial x^2} + \frac{\partial^2 u}{\partial y^2} = f(x, y) \tag{1}$$

$$B\{u(x, y)\} = g(x, y) \tag{2}$$

where B is an operator that is equal to 1 for the Dirichlet boundary, or $\partial/\partial n$ for the Neumann boundary with n being the co-ordinate normal to the boundary. Assume that there are N nodes, divided into N_i interior nodes and N_b boundary nodes. Let $\boldsymbol{r}_1, \boldsymbol{r}_2, \ldots, \boldsymbol{r}_{N_i}$ denote positions of interior nodes, and $\boldsymbol{r}_{N_i-1}, \boldsymbol{r}_{N_i-2}, \ldots, \boldsymbol{r}_N$ denote positions of boundary nodes. In the four collocation methods, $u(x, y)$ is approximated as follows:

$$\text{(A) } u(x, y) = \sum_{j=1}^{N} a_j \psi(x, y, x_j, y_j) \tag{3}$$

$$\text{(B) } u(x, y) = \sum_{j=1}^{N_i} a_j \left(\frac{\partial^2 \psi(x, y, x_j, y_j)}{\partial x^2} + \frac{\partial^2 \psi(x, y, x_j, y_j)}{\partial y^2} \right) + \sum_{j=N_i-1}^{N} a_j B\{\psi(x, y, x_j, y_j)\} \tag{4}$$

$$\text{(C) } u(x, y) = \sum_{j=1}^{N} a_j \psi(x, y, x_j, y_j) + \sum_{j=N-1}^{N+N_b} a_j \psi'(x, y, x_{j-N}, y_{j-N}) \tag{5}$$

$$\text{(D) } u(x, y) = \sum_{j=1}^{N} a_j \psi(x, y, x_j, y_j) + \sum_{j=1}^{N_b} b_j \phi(x, y, \xi_j, \eta_j) \tag{6}$$

DOI: 10.1002/cnm

where

$$\psi(x, y, x_j, y_j) = \sqrt{(x - x_j)^2 + (y - y_j)^2 + c^2} \tag{7}$$

$$\psi'(x, y, x_j, y_j) = \sqrt{(x - x_j)^2 + (y - y_j)^2 + d^2} \tag{8}$$

$$\phi(x, y, \xi_j, \eta_j) = \ln[(x - \xi_j)^2 + (y - \eta_j)^2] \tag{9}$$

and (ξ_j, η_j) are the co-ordinates of a source point located at a fictitious boundary outside the problem domain.

Method A is the multiquaric collocation method with straight collocation as proposed by Kansa [1]. Method B is the multiquaric collocation method with Hermite collocation, which was shown to produce more accurate solutions than method A in some cases [2, 3]. Method C is the multiquaric collocation method with additional collocation at the boundary, which was shown by Chantasiriwan to be more accurate than method A [4]. Method D is the method of fundamental solutions [5]. According to Equations (3)–(5), the vectors of solutions at interior nodes $\boldsymbol{u}_i$ and at boundary nodes $\boldsymbol{u}_b$ may be expressed as

$$\boldsymbol{u}_i = \boldsymbol{\Psi}_i \boldsymbol{a} \tag{10}$$

$$\boldsymbol{u}_b = \boldsymbol{\Psi}_b \boldsymbol{a} \tag{11}$$

Instead of using different symbols, the same symbols $\boldsymbol{\Psi}_i$, $\boldsymbol{\Psi}_b$ and $\boldsymbol{a}$ are used for methods A, B, and C with the understanding that they are different for different method. Collocating Equations (10) and (11) at interior and boundary nodes using Equations (1) and (2) results in

$$\begin{bmatrix} \nabla^2 \boldsymbol{\Psi}_i \\ B\{\boldsymbol{\Psi}_b\} \end{bmatrix} \boldsymbol{a} = \begin{bmatrix} \boldsymbol{f} \\ \boldsymbol{g} \end{bmatrix} \tag{12}$$

The solution vector $\boldsymbol{u}_i$ may also be expressed in terms of $\boldsymbol{f}$ and $\boldsymbol{g}$.

$$\boldsymbol{u}_i = \mathbf{C} \begin{bmatrix} \boldsymbol{f} \\ \boldsymbol{g} \end{bmatrix} \tag{13}$$

After solving Equation (12) for $\boldsymbol{a}$, inserting the result into Equation (10), and comparing the resulting equation with Equation (13), it can be seen that $\mathbf{C}$ is the solution of

$$\mathbf{C} \begin{bmatrix} \nabla^2 \boldsymbol{\Psi}_i \\ B\{\boldsymbol{\Psi}_b\} \end{bmatrix} = \boldsymbol{\Psi}_i \tag{14}$$

For method D, vectors of solutions ($\boldsymbol{u}_i$ and $\boldsymbol{u}_b$) may be expressed as

$$\boldsymbol{u}_i = \mathbf{H}_i \boldsymbol{a} + \mathbf{G}_i \boldsymbol{b} \tag{15}$$

$$\boldsymbol{u}_b = \mathbf{H}_b \boldsymbol{a} + \mathbf{G}_b \boldsymbol{b} \tag{16}$$

DOI: 10.1002/cnm

Collocating Equations (15) and (16) at interior and boundary nodes using Equations (1) and (2) results in

$$\nabla^2 \mathbf{H}_i \boldsymbol{a} = \boldsymbol{f} \tag{17}$$

$$B\{\mathbf{H}_b\}\boldsymbol{a} + B\{\mathbf{G}_b\}\boldsymbol{b} = \boldsymbol{g} \tag{18}$$

Solve Equations (17) and (18) for $\boldsymbol{a}$ and $\boldsymbol{b}$

$$\boldsymbol{a} = [\nabla^2 \mathbf{H}_i]^{-1}\boldsymbol{f} \tag{19}$$

$$\boldsymbol{b} = [B\{\mathbf{G}_b\}]^{-1}\{\boldsymbol{g} - B\{\mathbf{H}_b\}[\nabla^2 \mathbf{H}_i]^{-1}\boldsymbol{f}\} \tag{20}$$

The solution vector $\boldsymbol{u}_i$ may also be expressed in terms of $\boldsymbol{f}$ and $\boldsymbol{g}$.

$$\boldsymbol{u}_i = \mathbf{D}_1\boldsymbol{f} + \mathbf{D}_2\boldsymbol{g} \tag{21}$$

Comparing Equation (21) with the expression of $\boldsymbol{u}_i$ in terms of $\boldsymbol{f}$ and $\boldsymbol{g}$ from Equations (15), (19) and (20) gives equations for $\mathbf{D}_1$ and $\mathbf{D}_2$

$$\mathbf{D}_2 B\{\mathbf{G}_b\} = \mathbf{G}_i \tag{22}$$

$$\mathbf{D}_1 \nabla^2 \mathbf{H}_i = \mathbf{H}_i - \mathbf{D}_2 B\{\mathbf{H}_b\} \tag{23}$$

3. STOCHASTIC POISSON PROBLEM

If the source term and the boundary condition of the Poisson problem are stochastic, the Poisson problem will be stochastic. However, since the differential operator in Equation (1) does not change, the methods described in the previous section can be used to solve the stochastic Poisson problem. According to Equations (13) and (21), the solution at nodes i can be expressed as

$$u_i = \sum_{j=1}^{N} X_{i,j} f_j + \sum_{j=N_i+1}^{N} Y_{i,j} g_j \tag{24}$$

Let $\bar{f}(x_i, y_i)$ and $\bar{g}(x_i, y_i)$ be expected values of the source term and the boundary condition at node i. Random functions of the source term and the boundary condition are given by

$$f(x_i, y_i) = \bar{f}(x_i, y_i) + \varepsilon_1(x_i, y_i) \tag{25}$$

$$g(x_i, y_i) = \bar{g}(x_i, y_i) + \varepsilon_2(x_i, y_i) \tag{26}$$

where ε_1 and ε_2 are random errors. Assume that the probability density function for ε_1 and ε_2 is

$$p(\varepsilon) = \frac{1}{\sigma\sqrt{2\pi}} \exp\left[-\frac{1}{2}\left(\frac{\varepsilon}{\sigma}\right)^2\right] \tag{27}$$

so that the expected value and the variance of ε are zero and σ^2, respectively. This probability density function also implies that ε_1 and ε_2 at the same node are uncorrelated, and random errors at

DOI: 10.1002/cnm

different nodes are uncorrelated. Consequently, the expected value and the variance of the solution at node i are

$$E(u_i) = \sum_{j=1}^{N} X_{i,j} \bar{f}_j + \sum_{j=N_i+1}^{N} Y_{i,j} \bar{g}_j \tag{28}$$

$$\mathrm{Var}(u_i) = \left(\sum_{j=1}^{N} X_{i,j}^2 + \sum_{j=N_i+1}^{N} Y_{i,j}^2 \right) \sigma^2 \tag{29}$$

The normalized average variance may be defined as follows:

$$v = \frac{1}{N_i \sigma^2} \sum_{i=1}^{N_i} \mathrm{Var}(u_i) \tag{30}$$

If the exact solution in case of no random errors is available, and is not equal to zero, the average error may be computed from

$$e = \frac{1}{N_i} \sum_{i=1}^{N_i} \left(1 - \frac{E(u_i)}{u_{i,\mathrm{exact}}} \right)^2 \tag{31}$$

4. RESULTS AND DISCUSSION

Consider two test problems in a 1×1 square domain. There are 121 nodes distributed uniformly in the domain so that $N_i = 81$, $N_b = 40$, and grid spacing is 0.1. The fictitious boundary for method D is the perimeter of the concentric $s \times s$ square. N_b source points are evenly distributed on the fictitious boundary. In the first test problem, all four sides of the domain are subjected to the Dirichlet boundary condition. In the second test problem, the bottom and right sides of the domain are subjected to the Dirichlet boundary condition, whereas the top and left sides of the domain are subjected to the Neumann boundary condition. Let the exact solution in case of no random errors for both problems be

$$u_{\mathrm{exact}}(x, y) = \mathrm{e}^{x+y} \tag{32}$$

This solution can be used to generate $\bar{f}(x, y)$ and $\bar{g}(x, y)$. The values of e and v at each interior node can then be determined by the four methods as functions of the free parameters of methods A, B, and C, which are the shape parameters (c and d) of multiquadrics, and the free parameters of method D, which are the shape parameter and the fictitious boundary parameter (s). For method C, it is found that the value of the shape parameter d of function ψ' that yields the best performance is around $c - 0.2$ in both test problems. Therefore, this value is used to obtain the following results.

Figure 1 shows variations of average errors and normalized average variances of solutions to the first test problem by method A, B, and C. It can be seen that both errors and variances are quite sensitive to c. In comparing performances of the three methods, it should be reminded that a method is considered to perform better if its solution has both less error and less variance. The solution by method B is slightly more accurate than the solution by method A over the range of c between 0.31 and 0.84. However, the solution by method A has less variance over that range of c. It can then be concluded that, despite more complicate formulation, method B is not better than

DOI: 10.1002/cnm

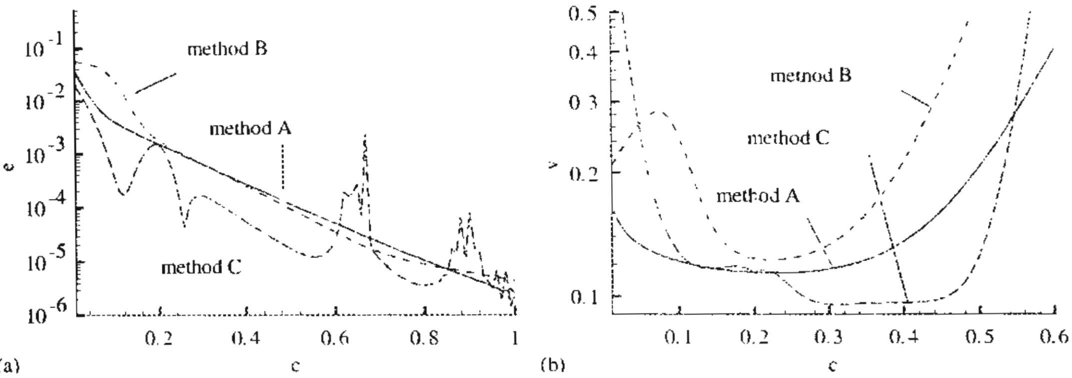

Figure 1. (a) Variations of average errors (e) with c for the solutions to the first test problem by methods A, B, and C; and (b) variations of normalized average variance (v) with c for solutions to the first test problem by methods A, B, and C.

method A. Comparison between method A and method C shows that method C can give a better solution than method A because there exists a range of c in which the solution by method C has less error and less variance than the solution by method A.

It has been recognized that the accuracy of the multiquadric collocation method depends on the shape parameter. Cheng *et al.* showed that the accuracy of the solution to a partial differential equation could be increased by reducing the shape parameter [6]. When c is too large, however, round-off error dominates, and the solution loses its accuracy. In order to maintain accuracy, computation must be performed with higher precision by a computer that has a higher computing power. Alternatively, the Contour-Pade algorithm [7] may be used. This algorithm enables stable computation of multiquadric interpolation for large values of shape parameter using a desktop computer. Larsson and Fornberg [8] used this algorithm in solving partial differential equations. Although using a large value of shape parameter may yield a very accurate solution, results in Figure 1 show that the solution is likely to be quite sensitive to random errors in inputs. If both the accuracy and the variance of the solution are taken into consideration, the recommended value of shape parameter should not be too large.

Variations of error and variance of the solution to the first test problem by method D as functions of c and s are shown in Figure 2. Error decreases almost monotonically with c until c is around 1.14 when a large condition number of the coefficient matrix results in instability. Variance is insensitive to c for the value of c between 0.01 and 1.0. Both error and variance are insensitive to s for the value of s between 1.4 and 4.6. Insensitivities of error and variance to free parameters of the solution by method D are considered to be an advantage of this method since this means that free parameters of the method may be chosen quite arbitrarily, whereas free parameters of methods A, B, and C may have to be chosen carefully to ensure optimal performance.

Solutions to the second test problem by methods A, B and C are compared in Figure 3. It can be seen that both errors and variances are quite sensitive to c. Method C is better than methods A and B in solving this problem because it yields the solution of less error and less variance for $c>0.23$. Method A is more accurate than method B when c is less than 0.39. Although method B is more accurate than method A when c is greater than 0.39, the variance of solution by method B is also greater. Therefore, method B cannot be considered to be better than method A in solving the

DOI: 10.1002/cnm

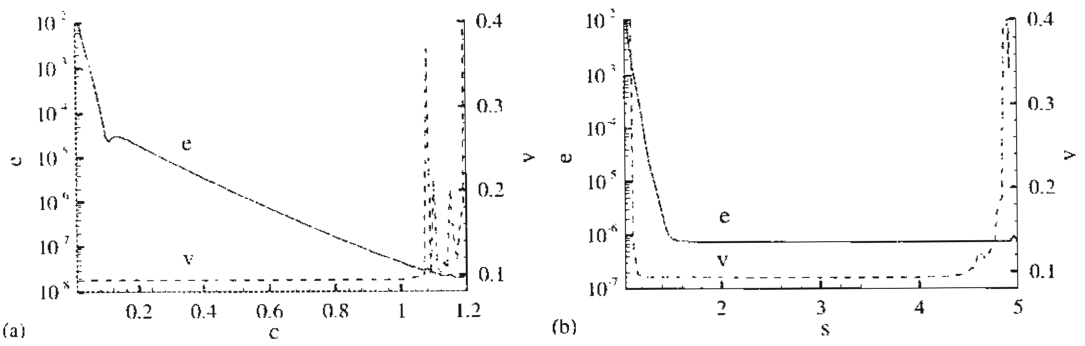

Figure 2. (a) Variations of average error (e) and normalized average variance (v) as functions of c for the solution to the first test problem by method D with $s = 2.0$; and (b) variations of average error (e) and normalized average variance (v) as functions of s for the solution to the first test problem by method D with $c = 0.6$.

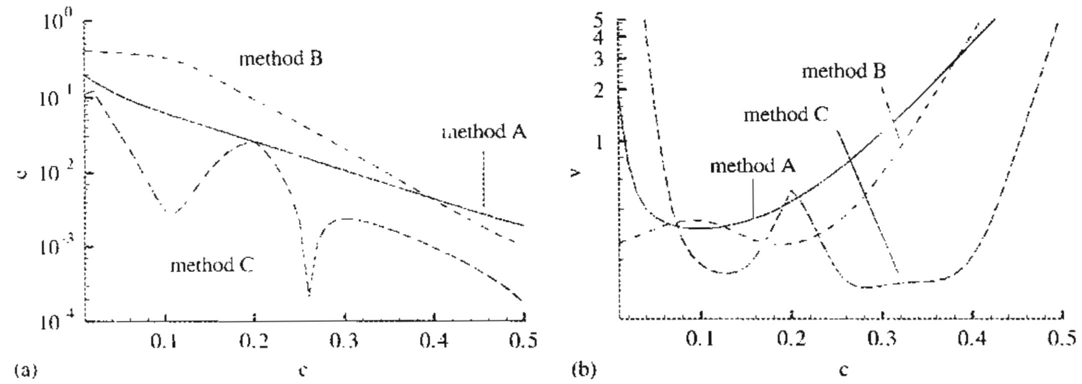

Figure 3. (a) Variations of average errors (e) with c for the solutions to the second test problem by methods A, B, and C; and (b) variations of normalized average variance (v) with c for the solutions to the second test problem by methods A, B, and C.

second problem. Previously, a comparison analysis found that the Hermite collocation (method B) outperformed the straight multiquadric collocation method (method A) [2]. Problems considered in that analysis were deterministic problems in which accuracy was the only concern. Results from Figures 1 and 3 show that the performance of method B in solving stochastic Poisson problems is not quite impressive.

In Figure 4(a), it is shown that the influence of c on the solution by method D in the second test problem is similar to the influence of c on the solution by method D in the first test problem. However, the solution to the second test problem has more error and more variance than the solution to the first test problem for the same values of c and s. Figure 4(b) shows that the variance of the solution is quite sensitive to s. The optimal value of s is between 1.9 and 2.6 since the solution is stable in this range, and both error and variance are not too large.

DOI: 10.1002/cnm

CNM 888

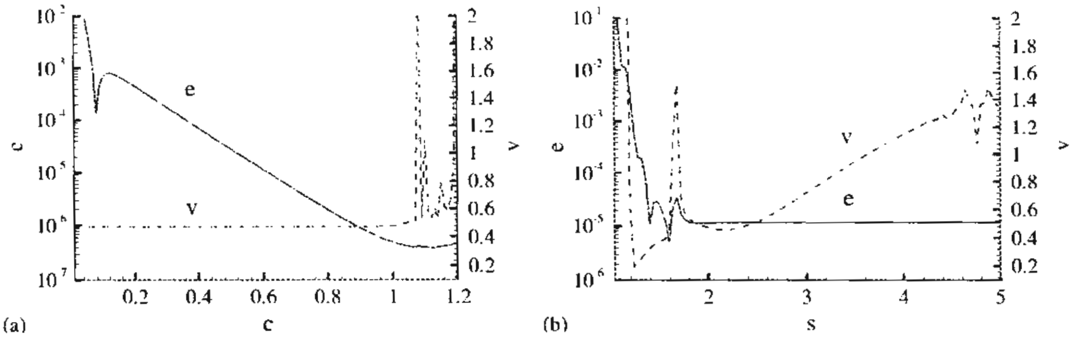

Figure 4. (a) Variations of average error (e) and normalized average variance (v) as functions of c for the solution to the second test problem by method D with $s=2.0$; and (b) variations of average error (e) and normalized average variance (v) as functions of s for the solution to the second test problem by method D with $c=0.6$.

Table I. Comparison of errors and variances of solutions to the first test problem by methods A, B, C, D and the finite difference method.

Method	e	v
A ($c=0.3$)	6.628×10^{-4}	0.1168
B ($c=0.3$)	6.707×10^{-4}	0.1338
C ($c=0.3$, $d=0.1$)	1.666×10^{-4}	0.09542
D ($c=0.6$, $s=2$)	7.372×10^{-7}	0.09331
FDM	8.006×10^{-5}	0.1044

Table II. Comparison of errors and variances of solutions to the second test problem by methods A, B, C, D and the finite difference method.

Method	e	v
A ($c=0.3$)	1.064×10^{-2}	1.109
B ($c=0.3$)	2.084×10^{-2}	0.6417
C ($c=0.3$, $d=0.1$)	2.408×10^{-3}	0.1410
D ($c=0.6$, $s=2$)	1.148×10^{-5}	0.4700
FDM	7.599×10^{-4}	0.1330

The finite difference method provides the benchmark solutions to the first and the second test problems with which the solutions by methods A, B, C and D may be compared. In Tables I and II, parameters of the four methods are chosen so that no other parameters give solutions that have lower errors and lower variances than the chosen parameters. It can be seen that FDM performs better than methods A, B and C. However, method D performs better than FDM in

DOI: 10.1002/cnm

solving the first test problem. The performances of method D and FDM in solving the second test problem are comparable.

Since only two problems are used to test the four collocation methods in this paper, a rigorous analysis will be needed before it can be concluded that method C performs better than methods A and B, and that method D performs better than method C in solving general partial differential equations. In the meantime, there are reasons to believe that analogous results will be obtained when the four collocation methods are used to solve other linear partial differential equations. In a paper by Fornberg *et al.* [9], it was shown that adding collocation nodes near the boundary could improve the collocation method. Although method C does not require additional collocation nodes near the boundary, it does require additional basis functions. The reason why methods A and B do not perform as well as method C may be attributed to the fact that methods A and B use fewer basis functions than method C. However, the number of basis functions is not the only factor that determine the performance of a collocation method. Despite having the same number of basis functions, method D is apparently better than method C because some of basis functions in method D are fundamental solutions to the Poisson problem, whereas all basis functions in method C are multiquadrics. Results from this study agree with those from a previous study by Chantasiriwan [4], which shows that the method of fundamental solutions performs better than collocation methods that use multiquadrics as basis functions.

5. CONCLUSIONS

The quality of a solution to a stochastic Poisson problem depends on both its accuracy and its variance. Four methods presented in this paper are formulated so that the expression for the solution is given in terms of the source term and the boundary condition. Results from two test problems reveal that although a large value of the shape parameter of multiquadrics may yield an accurate solution, the solution may also be too sensitive to random errors in inputs. Furthermore, it is found that the multiquadric collocation method with addition collocation at boundary outperforms both the straight multiquadric collocation and the multiquadric collocation method with Hermite collocation because it can yield a solution of lower error and variance. The method of fundamental solutions is found to outperform all multiquadric collocation methods.

ACKNOWLEDGEMENTS

This research has been financially supported by the Thailand Research Fund.

REFERENCES

1. Kansa EJ. Multiquadrics—a scattered data approximation scheme with applications to computational fluid-dynamics—II solutions to parabolic, hyperbolic and elliptic partial differential equations. *Computers and Mathematics with Applications* 1990; **19**(8–9):147–161.
2. Power H, Barraco V. A comparison analysis between unsymmetric and symmetric radial basis function collocation methods for the numerical solution of partial differential equations. *Computers and Mathematics with Applications* 2002; **43**(3–5):551–583.
3. La Rocca A, Rosales AH, Power H. Radial basis function Hermite collocation approach for the solution of time dependent convection–diffusion problems. *Engineering Analysis with Boundary Elements* 2005; **29**(4):359–370.

DOI: 10.1002/cnm

4. Chantasiriwan S. Cartesian grid methods using radial basis functions for solving Poisson, Helmholtz, and diffusion–convection equations. *Engineering Analysis with Boundary Elements* 2004; **28**(12):1417–1425.
5. Golberg MA. The method of fundamental solutions for Poisson's equations. *Engineering Analysis with Boundary Elements* 1995; **16**(3):205–213.
6. Cheng AHD, Golberg MA, Kansa EJ, Zammito Q. Exponential convergence and H-*c* multiquadric collocation method for partial differential equations. *Numerical Methods for Partial Differential Equations* 2003; **19**(5):571–594.
7. Fornberg B, Wright G. Stable computation of multiquadric interpolants for all values of the shape parameter. *Computers and Mathematics with Applications* 2004; **48**(5–6):853–867.
8. Larsson E, Fornberg B. A numerical study of some radial basis function based solution methods for elliptic PDEs. *Computers and Mathematics with Applications* 2003; **46**(5–6):891–902.
9. Fornberg B, Driscoll TA, Wright G, Charles R. Observations on the behavior of radial basis function approximations near boundaries. *Computers and Mathematics with Applications* 2002; **43**(3–5):473–490.

DOI: 10.1002/cnm

Multiquadric Collocation Method for Time-dependent Heat Conduction Problems with Temperature-dependent Thermal Properties

Somchart Chantasiriwan
Faculty of Engineering, Thammasat University, Pathum Thani 12121, Thailand
Phone: 66-(0)-25643001, E-mail: somchart@engr.tu.ac.th

ABSTRACT

The multiquadric collocation method is a meshless method that uses multiquadrics as its basis function. Problems of nonlinear time-dependent heat conduction in materials having temperature-dependent thermal properties are solved by using this method and the Kirchhoff transformation. Variable transformation is simplified by assuming that thermal properties are piecewise linear functions of temperature. The resulting nonlinear equation is solved by an iterative scheme. The multiquadric collocation method is tested by a heat conduction problem for which the exact solution is known. Results indicate satisfactory performance of the method.

Key Words: Kirchhoff transformation, meshless, radial basis function

Introduction

Multiquadrics is a radial basis function discovered by Hardy [1]. The multiquadric collocation method, also known as the Kansa's method [2], has been used to solve various steady-state problems [3-6] and time-dependent problems [7-9] in mechanics. It has been shown that this method can yield satisfactory solutions to linear problems. Being a meshless method, this method has advantages over conventional numerical methods such as the finite element method and the finite difference method. However, before considering the multiquadric collocation method as a serious alternative to the finite element method and the finite difference method, this method must be tested with nonlinear time-dependent problems. There have been relatively few such problems solved by the multiquadric collocation method [10, 11].

A well-known nonlinear time-dependent problem is the time-dependent heat conduction problem with temperature-dependent thermal properties. Several algorithms have been proposed to find its solution. Previous algorithms, however, depend on mesh-dependent methods such as the finite element method and the finite difference method. In this paper, an algorithm making use of the multiquadric collocation method is proposed. First, the problem is simplified by the Kirchhoff transformation. Then the multiquadric collocation method is formulated to deal with the problem in an iterative manner. The proposed algorithm is used to solve heat conduction problems in a fictitious material. Results show that solutions for problems in which heat capacities and thermal conductivities are piecewise linear functions of temperature are satisfactorily accurate.

Heat Conduction Problem

Heat conduction phenomena in which heat capacities and thermal conductivities depend on temperature are described by the following partial differential equation.

$$\rho c_p(T)\frac{\partial T}{\partial t} \quad = \quad \vec{\nabla}\left(k(T)\vec{\nabla}T\right)+s(\vec{r},t) \qquad \text{for } \vec{r} \text{ in } \Omega \qquad (1)$$

Without the loss of generality, density is assumed to be constant. In addition, initial and boundary conditions are given by

$$T(\vec{r},0) = T_0(\vec{r}) \qquad \text{for } \vec{r} \text{ in } \Omega \tag{2}$$

$$T(\vec{r},t) = T_b(\vec{r},t) \qquad \text{for } \vec{r} \text{ on } \Gamma_1 \tag{3}$$

$$k(T)\frac{\partial T}{\partial n} = q_b(\vec{r},t) \qquad \text{for } \vec{r} \text{ on } \Gamma_2 \tag{4}$$

Define u by using the Kirchhoff transformation.

$$u(\vec{r},t) = \int_{T_r}^{T} k(T)dT \tag{5}$$

Transform the dependent variable in Eqs. (1) – (4) from T to u.

$$\gamma(u)\frac{\partial u}{\partial t} = \nabla^2 u + s(\vec{r},t) \qquad \text{for } \vec{r} \text{ in } \Omega \tag{6}$$

$$u(\vec{r},0) = u_0(\vec{r}) \qquad \text{for } \vec{r} \text{ in } \Omega \tag{7}$$

$$u(\vec{r},t) = u_b(\vec{r},t) \qquad \text{for } \vec{r} \text{ on } \Gamma_1 \tag{8}$$

$$\frac{\partial u}{\partial n} = q_b(\vec{r},t) \qquad \text{for } \vec{r} \text{ on } \Gamma_2 \tag{9}$$

where $\gamma = \rho c_p/k$ is the reciprocal of thermal diffusivity α.

Discretization Scheme

Consider thermal properties of three materials shown in Tables 1, 2 and 3. Thermal conductivities and heat capacities of materials A, B, and C are the same as those of zirconium, tungsten, and tantalum, respectively, which are obtained from ref. [12]. However, the densities of materials A, B, and C are constant instead of temperature-dependent as the actual densities of zirconium, tungsten, and tantalum are. It can be seen that thermal conductivities of these materials are not linear functions of T. Equation (5) indicates that $u(T)$ is a monotonically increasing function because $k(T)$ is always positive, and an explicit function $u(T)$ can be found quite easily no matter how complicated $k(T)$ is. On the contrary, an explicit function of $T(u)$ is difficult to determine unless $k(T)$ is a linear function. Therefore, although it is possible to approximate $k(T)$ as a sixth-order polynomial function of T using data from 7 temperatures, it is more efficient for computational purpose to approximate $k(T)$ as a piecewise linear function:

$$k(T) = k_{i-1} + \left(\frac{k_i - k_{i-1}}{T_i - T_{i-1}}\right)(T - T_{i-1}) \qquad (T_{i-1} \le T < T_i) \tag{10}$$

where T_1, T_2, …, T_7 are 7 temperatures in Tables 1 – 3 in the ascending order, and k_1, k_2, …, k_7 are the corresponding thermal conductivities. Let T_r = 100 K. Substituting $k(T)$ from Eq. (10) into Eq. (5) yields

$$u(T) = u_{i-1} + k_{i-1}(T - T_{i-1}) + \frac{1}{2}\left(\frac{k_i - k_{i-1}}{T_i - T_{i-1}}\right)(T - T_{i-1})^2 \qquad (T_{i-1} \le T < T_i) \tag{11}$$

from which the inversion formula for $T(u)$ can be obtained as follows.

$$T(u) = T_{i-1} + \left(\frac{T_i - T_{i-1}}{k_i - k_{i-1}}\right)\left[-k_{i-1} + \sqrt{k_{i-1}^2 + 2\left(\frac{k_i - k_{i-1}}{T_i - T_{i-1}}\right)(u - u_{i-1})^2}\right] \qquad (u_{i-1} \le u < u_i) \tag{12}$$

After values of u corresponding to 7 temperatures in Tables 1 – 3 for each material are calculated, and γ can be plotted as functions of u. Figure 1 shows that, for each material, γ does not vary rapidly with u, and can be approximated as a piecewise linear function. It is interesting to note that variations of γ with u for the three materials are quite different.

Discretization of Eqs. (6) – (9) yields

$$\gamma^*\left(\frac{u_i^{(n)} - u_i^{(n-1)}}{\Delta t}\right) = \theta\nabla^2 u_i^{(n)} + (1-\theta)\nabla^2 u_i^{(n-1)} + s(\vec{r}_i,(n-1+\theta)\Delta t) \quad (13)$$

$$u_i^{(0)} = u_0(\vec{r}_i) \quad (14)$$

$$u_i^{(n)} = u_b(\vec{r}_i, n\Delta t) \quad (15)$$

$$\frac{\partial u_i^{(n)}}{\partial n} = q_b(\vec{r}_i, n\Delta t) \quad (16)$$

whrere

$$\gamma^* = \gamma\left(\theta u_i^{(n)} + (1-\theta)u_i^{(n-1)}\right) \quad (17)$$

Relaxation parameter θ must be greater than 0. In this study, $\theta = 0.5$.

Multiquadric Collocation Method

Let $\vec{r}_i$ ($i = 1, 2, \ldots, N_b$) denote positions of boundary nodes, and $\vec{r}_i$ ($i = N_b + 1, N_b + 2, \ldots, N_b + N_i$) denote positions of interior nodes. The multiquadric collocation method approximates u as a linear combination of radial basis functions ϕ.

$$u(\vec{r}, n\Delta t) = \sum_{j=1}^{N_b+N_i} a_j^{(n)}\phi(|\vec{r} - \vec{r}_j|) \quad (18)$$

where

$$\phi(r) = \sqrt{r^2 + c^2} \quad (19)$$

is known as multiquadrics. This function contains the shape parameter c. A suitable value of c is to be found by numerical experiments in this paper. Coefficients $a_j^{(0)}$ are determined directly from collocation using Eq. (14).

$$\sum_{j=1}^{N_b+N_i} a_j^{(0)}\phi(|\vec{r}_i - \vec{r}_j|) = u_0(\vec{r}_i) \qquad (i = 1, 2, \ldots, N_b + N_i) \quad (20)$$

Coefficients $a_j^{(n)}$ ($n \geq 1$) must be determined iteratively. First, Eq. (13) is rearranged.

$$\theta\nabla^2 u_i^{(n)} - \left(\frac{\gamma^*}{\Delta t}\right)u_i^{(n)} = -(1-\theta)\nabla^2 u_i^{(n-1)} - \left(\frac{\gamma^*}{\Delta t}\right)u_i^{(n-1)} - s(\vec{r}_i,(n-1+\theta)\Delta t) \quad (21)$$

Next substitute $u_i^{(n)}$ and $u_i^{(n-1)}$ from Eq. (18) into Eqs. (21), (15), and (16).

$$\theta\sum_{j=1}^{N_b+N_i} a_j^{(n)}\nabla_i^2\phi(|\vec{r}_i - \vec{r}_j|) - \left(\frac{\gamma^*}{\Delta t}\right)\sum_{j=1}^{N_b+N_i} a_j^{(n)}\phi(|\vec{r}_i - \vec{r}_j|) =$$

$$-(1-\theta)\sum_{j=1}^{N_b+N_i} a_j^{(n-1)}\nabla_i^2\phi(|\vec{r}_i - \vec{r}_j|) - \left(\frac{\gamma^*}{\Delta t}\right)\sum_{j=1}^{N_b+N_i} a_j^{(n-1)}\phi(|\vec{r}_i - \vec{r}_j|) - s(\vec{r}_i,(n-1+\theta)\Delta t)$$

$$(i = N_b + 1, N_b + 2, \ldots, N_b + N_i) \quad (22)$$

$$\sum_{j=1}^{N_b+N_i} a_j^{(n)} \phi\left(\left|\vec{r}_i - \vec{r}_j\right|\right) \quad = \quad u_b\left(\vec{r}_i, n\Delta t\right) \qquad (i = 1, 2, \ldots, N_{b1}) \tag{23}$$

$$\sum_{j=1}^{N_b+N_i} a_j^{(n)} \frac{\partial \phi}{\partial n} \quad = \quad q_b\left(\vec{r}_i, n\Delta t\right) \qquad (i = N_{b1} + 1, N_{b1} + 2, \ldots, N_{b1} + N_{b2}) \tag{24}$$

Initially, it must be assumed that $a_j^{(n)} = a_j^{(n-1)}$ so that γ^* can be determined, and Eqs. (22) – (24) can be solved for $a_j^{(n)}$. After the determination of $a_j^{(n)}$, Eqs. (22) – (24) are solved for new values of $a_j^{(n)}$. The iteration process continues until the average difference between new and old values of $u_i^{(n)}$ is less than a tolerance number δ.

$$\left[\frac{1}{N_i} \sum_{i=N_b+1}^{N_b+N_i} \left(1 - \frac{\left(u_i^{(n)}\right)_{\text{new}}}{\left(u_i^{(n)}\right)_{\text{old}}}\right)^2\right]^{1/2} \quad < \quad \delta \tag{25}$$

provided that no value of $u_i^{(n)}$ is zero. Otherwise, a new measure of the difference between new and old values of $u_i^{(n)}$ must be used. In this study, $\delta = 1.0 \times 10^{-5}$.

After converged values of $u_i^{(n)}$ have been found, $T_i^{(n)}$ can be determined from Eq. (12). If exact temperatures are known, average error in computed temperatures (ε) can be found from the average difference between computed temperatures and exact temperatures at N_t test nodes, of which locations are denoted by $\vec{\xi}_i$ ($i = 1, 2, \ldots, N_t$).

$$\varepsilon \quad = \quad \left[\frac{1}{N_t} \sum_{i=1}^{N_t} \left(1 - \frac{T_i^{(n)}}{\left(T_i^{(n)}\right)_{\text{exact}}}\right)^2\right]^{1/2} \tag{26}$$

where $T_i^{(n)}$ is determined from

$$u_i^{(n)} \quad = \quad \sum_{j=1}^{N_b+N_i} a_j^{(n)} \phi\left(\left|\vec{\xi}_i - \vec{r}_j\right|\right) \tag{27}$$

using Eq. (12), and $\left(T_i^{(n)}\right)_{\text{exact}}$ is the exact solution at location $\vec{\xi}_i$ and time $n\Delta t$.

Results and Discussion

Consider a 0.12 m × 0.12 m square domain having the thermal properties of material A. Let N nodes be uniformly distributed in the domain so that there are $(\sqrt{N} - 2)^2$ interior nodes and $(4\sqrt{N} - 4)$ boundary nodes. The spacing between two adjacent nodes is, therefore, $0.12/(\sqrt{N} - 1)$ m, which is denoted by Δ. Coordinates of N nodes are $((i-1)\Delta, (j-1)\Delta)$, where i and j run from 1 to $\sqrt{N}$. As shown in Fig. 2, the bottom, right, and top sides of the domain are subjected to the Dirichlet boundary condition, whereas the left side of the domain is subjected to the Neumann boundary condition. The exact solution is

$$T_{\text{exact}}(x, y, t) \quad = \quad [104.43 + 4.43\cos(0.01t)].\exp[10(x + y)] \tag{28}$$

so that the minimum and maximum values are approximately 100 K and 1200 K, respectively, which are the lower and upper limits of the temperature range in Tables 1 – 3. This function is used to generate the initial value function $T_0(x, y)$, the Dirichlet boundary value function $T_b(x, y, t)$, the Neumann boundary value function $q_b(x, y, t)$ function, and the source function $s(x, y, t)$ according to

$$s(x, y, t) = \rho c(T)\frac{\partial T}{\partial t} - k(T)\left(\frac{\partial^2 T}{\partial x^2} + \frac{\partial^2 T}{\partial y^2}\right) - \frac{dk}{dT}\left[\left(\frac{\partial T}{\partial x}\right)^2 + \left(\frac{\partial T}{\partial y}\right)^2\right] \tag{29}$$

The multiquadric collocation method is then used to obtain an approximate solution, which can be compared with the exact solution to evaluate the performance of the method.

Effects of shape parameter. It is well known that the accuracy of the multiquadric collocation method is sensitive to the shape parameter, which may be chosen to optimize the performance of multiquadrics as an interpolating function. Although a variable shape parameter has been suggested [13, 14], there is an evidence that using a variable shape parameter does not always lead to a more accurate solution than using a constant shape parameter [7]. In order to investigate effects of the shape parameter on solution by the proposed method, variations with time of average error are calculated for 5 values of the shape parameter (0.1, 0.11, 0.12, 0.13, and 0.14). Coordinates of 36 interior test nodes are $(0.02i - 0.01, 0.02j - 0.01)$, where i and j run from 1 to 6, $N = 49$, and $\Delta t = 0.5$ s. Figure 3 shows that average error depends on the shape parameter. It is obvious that there exists an optimum value of shape parameter as far as accuracy is concerned. For material A, the optimum value is around 0.11. It is also found that the optimum values for material B and C are 0.11 and 0.14, respectively. Instead of proposing an algorithm for finding the optimum value, it is proposed that the value of 0.12 is an appropriate value since this value gives a solution that is not much less accurate than the solution at the optimum value of shape parameter.

Convergence test. Behaviors of solutions by the multiquadric collocation method as Δ and Δt decrease are investigated by using three values of N. With $\Delta t/\Delta^2$ kept constant at 1250 s/m^2, values of $(\Delta, \Delta t)$ corresponding $N = 25$, 49, and 169 are (0.03 m, 1.125 s), (0.02 m, 0.5 s), and (0.01 m, 0.125 s), respectively. The shape parameter is varied according to $c/\Delta = 6$. Wong et al. [8] and Fasshauer [15] also suggested that c should be proportional to Δ. Results in Fig. 4 indicate that reducing Δ and Δt in the multiquadric collocation method results in a more accurate solution.

Effects of random node arrangement. The multiquadric collocation method does not require a uniform arrangement of nodes like the finite difference method. In fact, a random arrangement may be preferable if it makes the process of node placement easier. A random node arrangement results from distributing each interior node i randomly according to $(x_i, y_i) = (\bar{x}_i + d_1\Delta,\ \bar{y}_i + d_2\Delta)$, where $(\bar{x}_i, \bar{y}_i)$ is the position of node i in the uniform arrangement, and d_1 and d_2 are random numbers between –0.5 and 0.5. The result for the uniform arrangement is compared with results for 5 random arrangements with $N = 49$, $\Delta t = 0.5$ s, and $c = 0.12$. Figure 5 shows that a random node arrangement does not significantly affect the accuracy of the solution.

Boundary solution. Boundary solution by a collocation method may be less accurate than interior solution. Figure 6 compares average error for the 36 interior test nodes used to obtain Figs. 3 – 5 with average error for 6 boundary test nodes on Γ_2 as shown in Fig. 2. It can be seen that boundary solution is slightly less accurate than interior solution. In addition, Fig. 6 shows variation of average error in heat flux (ε_q) for 18 test nodes on Γ_1 as shown in Fig. 2.

$$\varepsilon_q = \left[\frac{1}{N_t}\sum_{i=1}^{N_t}\left(1-\frac{q_i^{(n)}}{\left(q_i^{(n)}\right)_{exact}}\right)^2\right]^{1/2} \tag{30}$$

where

$$q_i^{(n)} = \sum_{j=1}^{N_b+N_i} a_j^{(n)}\frac{\partial\phi}{\partial n}\left(\left|\vec{\xi}_i-\vec{r}_j\right|\right) \tag{31}$$

and $\left(q_i^{(n)}\right)_{exact}$ is the exact heat flux at boundary location $\vec{\xi}_i$ and time $n\Delta t$. Average error in computed heat flux is about one order of magnitude larger than average error in computed temperatures.

Comparison with the finite difference method. The finite difference method can be considered as a benchmark with which meshless methods such as the multiquadric collocation method should be compared. Although meshless methods have an advantage over the finite difference method in that an arbitrary problem geometry can be easily dealt with, this advantage should not mean solution accuracy has to be compromised. Figure 7 compares the solution to the test problem by the finite difference method having $N = 169$ and $\Delta t = 0.125$ s with the solution by the multiquadric collocation method having $N = 169$, $\Delta t = 0.125$ s, and $c = 0.06$. Coordinates of the 121 test nodes used for computing both solutions are ($0.01i$, $0.01j$), where i and j run from 1 to 11. It is evident that both methods yield solutions of comparable accuracy. It is interesting to note, however, that comparison performed using 3.0 GHz Pentium 4 CPU indicated that the finite difference method was a little faster because it used less CPU time (116.95 seconds) than the multiquadric collocation method (134.55 seconds).

Conclusions

Heat conduction problems in materials of which thermal properties are temperature-dependent can be solved by the multiquadric collocation method. Results show that the shape parameter of multiquadrics affects the accuracy of the solution. A value of the shape parameter that yields solutions of satisfactory accuracy is suggested. In addition, it is shown that the multiquadric collocation method is more accurate as grid spacing and time step decrease, a random arrangement of nodes does not affect the accuracy of the method significantly, average error in computed heat flux is about an order of magnitude larger than average error in computed temperatures, and solutions by the multiquadric collocation method and the finite difference method have comparable accuracy.

It has been accepted that meshless methods have advantages over the finite difference method and the finite element method in their ability to deal with domains of complex geometry without requiring mesh generation. Acceptance of these methods depends on more testing of these methods using nonlinear time-dependent problems. This paper has shown that the multiquadric collocation method has the potential to be an acceptable alternative numerical method for solving general partial differential equations.

Acknowledgment

The author would like to acknowledge the financial support from the Thailand Research Fund.

Nomenclature

a	=	coefficient
c	=	shape parameter
c_p	=	heat capacity, J/(kg.K)
d_1, d_2	=	random numbers
k	=	thermal conductivity, W/(m.K)
N	=	number of nodes
n	=	normal coordinate or time level
q	=	heat flux, W/m^2
r	=	distance between two nodes, m
$\vec{r}$	=	position vector of a boundary or an interior node
s	=	source function
T	=	temperature, K
t	=	time, s
u	=	Kirchhoff transformation variable, W/m
x	=	horizontal coordinate, m
y	=	vertical coordinate, m
Greek symbols		
Δ	=	grid spacing, m
Δt	=	time step, s
δ	=	tolerance number
ε	=	average error in computed temperature
ε_q	=	average error in computed heat flux
ϕ	=	multiquadrics
Γ_1	=	Dirichlet boundary
Γ_2	=	Neumann boundary
γ	=	reciprocal of thermal diffusivity, s/m^2
θ	=	relaxation parameter
ρ	=	density, kg/m^3
Ω	=	domain
$\vec{\xi}$	=	position vector of a test node
Subscripts		
0	=	initial value
b	=	boundary
i	=	position index or interior
j	=	position index
r	=	reference
t	=	test

Superscript

n = time index

References

[1] Hardy, R. L., 1971, "Multiquadric equations of topography and other irregular surfaces," Journal of Geophysical Research **176**, pp. 1905-1915.

[2] Kansa, E. J., 1990, "Multiquadrics – A scattered data approximation scheme with applications to computational fluid dynamics II," Computer and Mathematics with Applications **19**, pp. 147-161.

[3] Leitao, V. M. A., 2001, "A meshless method for Kirchhoff plate bending problem," International Journal for Numerical Methods in Engineering **52**, pp. 1107-1130.

[4] Power, H. and Barraco, 2002, "A comparison analysis between unsymmetric and symmertic radial basis function collocation methods for the numerical solution of partial differential equations," Computer and Mathematics with Applications **43**, pp. 551-583.

[5] Li, J., Cheng. A. H. D., and Chen, C. S., 2003, "A comparison of efficiency and error convergence of multiquadric collocation method with finite element method," Engineering Analysis with Boundary Elements **26**, pp. 205-255.

[6] Chantasiriwan, S., 2004, "Cartesian grid methods using radial basis functions for solving Poisson, Helmholtz, and diffusion–convection equations," Engineering Analysis with Boundary Elements **28**, pp. 1417-1425.

[7] Zerroukat, M., Power, H., and Chen C. S., 1998, "A numerical method for heat transfer problems using collocation and radial basis functions," International Journal for Numerical Methods in Engineering **42**, pp. 1263-1278.

[8] Wong, A. S. M., Hon, Y. C., Li, T. S., Chung, S. L., and Kansa, E. J., 1999, "Multizone decomposition for simulation of time-dependent problems using the multiquadric scheme," Computer and Mathematics with Applications **37**, pp. 23-43.

[9] Ferreira, A. J. M., Martins, P. A. L. S., and Roque, C.M.C., 2005, "Solving time-dependent engineering problems with multiquadrics," Journal of Sound and Vibration **280**, pp. 595-610.

[10] Sarra, S. A., 2005, "Adaptive radial basis function methods for time dependent partial differential equations," Applied Numerical Mathematics **54**, pp. 79-94.

[11] Hon, Y. C., and Mao, X. Z., 1998, "An efficient numerical scheme for Burgers' equation," Applied Mathematics and Computation **95**, pp. 37-50.

[12] Incropera, F. P., and DeWitt, D. P., 1996, *Introduction to Heat Transfer*, John Wiley and Sons, New York.

[13] Carlson, R. E. and Foley, T. A., 1991, "The parameters R2 in multiquadric interpolation," Computer and Mathematics with Applications **21**, pp. 29-42.

[14] Kansa, E. J. and Carlson, R. E., 1992, "Improved accuracy of multiquadric interpolation using variable shape parameters," Computer and Mathematics with Applications **24**, pp. 99-120.

[15] Fasshauer, G. E., 2002, "Newton iteration with multiquadrics for the solution of nonlinear PDEs," Computer and Mathematics with Applications **43**, pp. 423-438.

TABLE CAPTIONS

Table 1	Thermal properties of material A
Table 2	Thermal properties of material B
Table 3	Thermal properties of material C

FIGURE CAPTIONS

Figure 1	Variations of the reciprocal of thermal diffusivities of materials A, B, and C with Kirchhoff transformation variable.
Figure 2	Domain of test problem is a 0.12 m × 0.12 m square. The left side is the Neumann boundary, and the other three sides are the Dirichlet boundary. Black circles indicate locations of 24 boundary test nodes.
Figure 3	Variations with time of average error for 36 interior test nodes corresponding to different shape parameters of multiquadrics.
Figure 4	Variations with time of average error for 36 interior test nodes corresponding to different grid spacings and time steps.
Figure 5	Variations with time of average error for 36 interior test nodes corresponding to different node arrangements. The solid line represents the uniform arrangement, whereas five other lines represent five random arrangements.
Figure 6	Comparison of average error in computed temperatures for 36 interior test nodes, average error in computed temperatures for 6 boundary test nodes, and average error in computed heat flux for 18 boundary test nodes.
Figure 7	Comparison of average errors for 121 interior test nodes by the multiquadric collocation method (MCM) and the finite difference method (FDM).

Table 1

T (K)	ρ (kg.m^{-3})	k (W.m^{-1}.K^{-1})	c (J.kg^{-1}.K^{-1})
100	19300	208	87
200	19300	186	122
400	19300	159	137
600	19300	137	142
800	19300	125	145
1000	19300	118	148
1200	19300	113	152

Table 2

T (K)	ρ (kg.m^{-3})	k (W.m^{-1}.K^{-1})	c (J.kg^{-1}.K^{-1})
100	6570	33.2	205
200	6570	25.2	264
400	6570	21.6	300
600	6570	20.7	322
800	6570	21.6	342
1000	6570	23.7	362
1200	6570	26	344

Table 3

T (K)	ρ (kg.m^{-3})	k (W.m^{-1}.K^{-1})	c (J.kg^{-1}.K^{-1})
100	5000	90	420
200	5000	100	400
400	5000	120	360
600	5000	140	320
800	5000	160	280
1000	5000	180	240
1200	5000	200	200

Figure 1

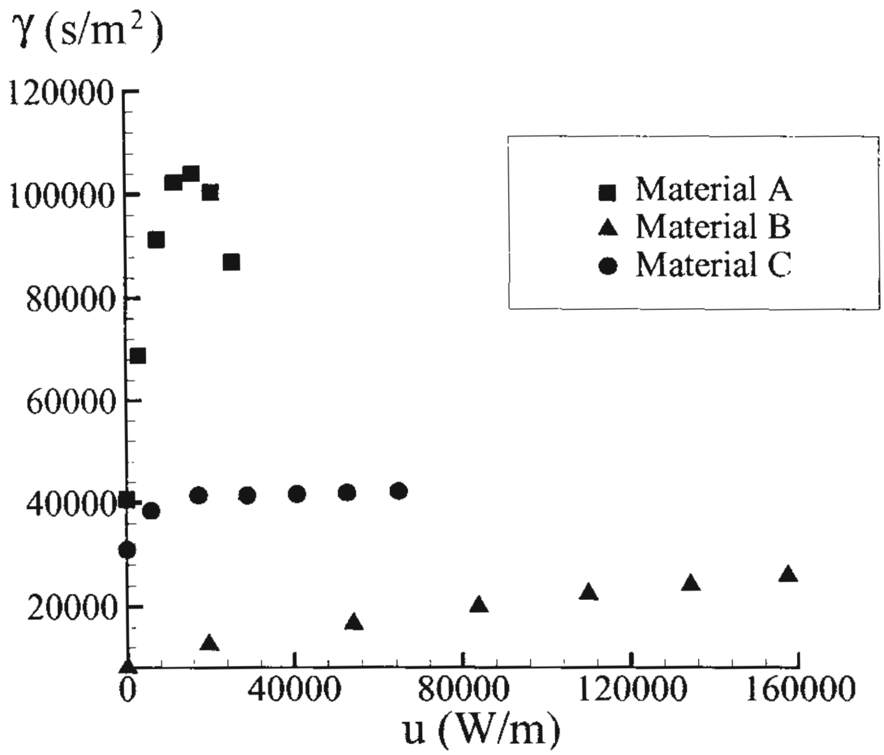
γ (s/m²)
120000
100000
80000
60000
40000
20000
0
40000
80000
120000
160000
u (W/m)
Material A
Material B
Material C

Figure 2

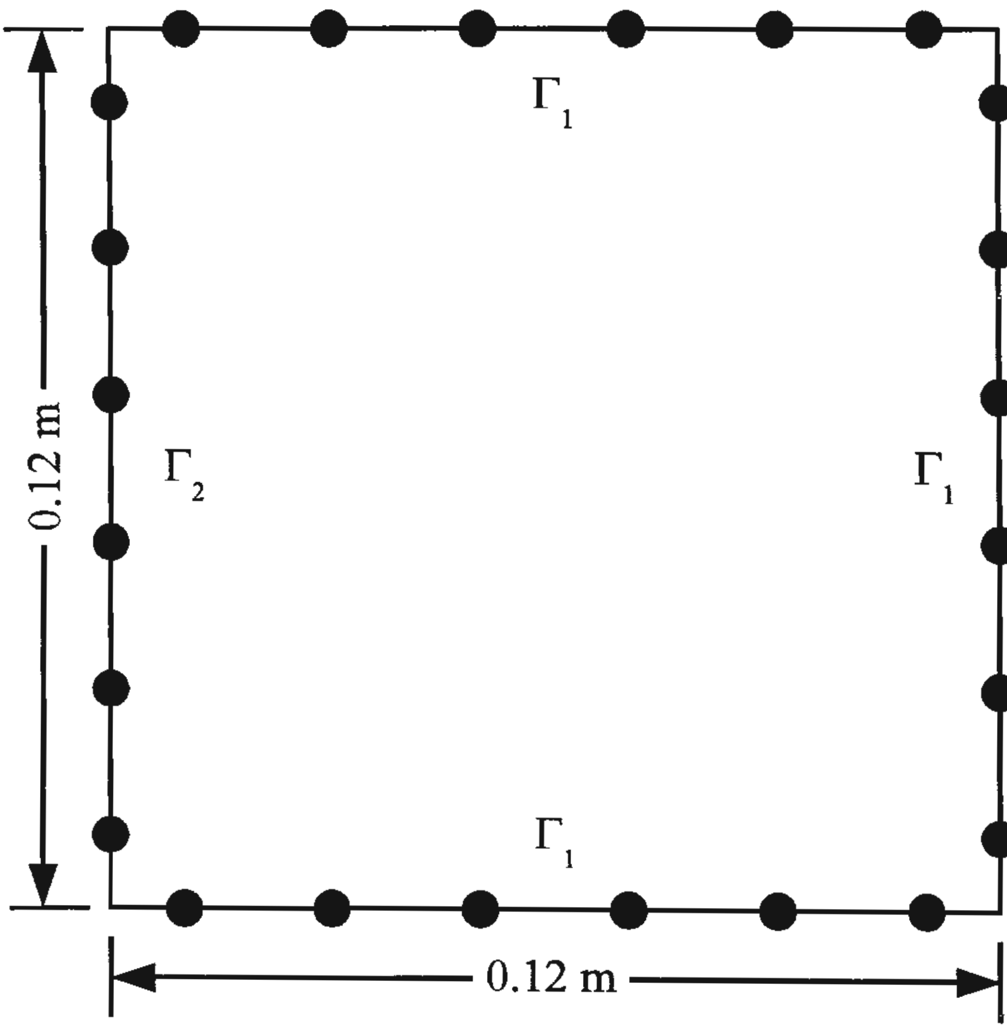

Figure 3

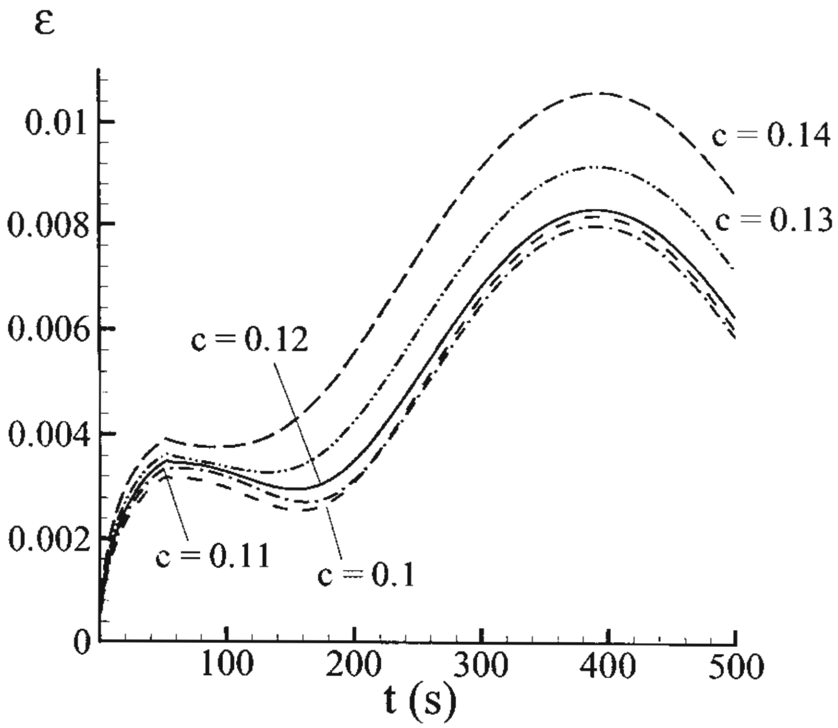
ε
0.01
0.008
0.006
0.004
0.002
0
100
200
300
400
500
t (s)
c = 0.14
c = 0.13
c = 0.12
c = 0.11
c = 0.1

Figure 4

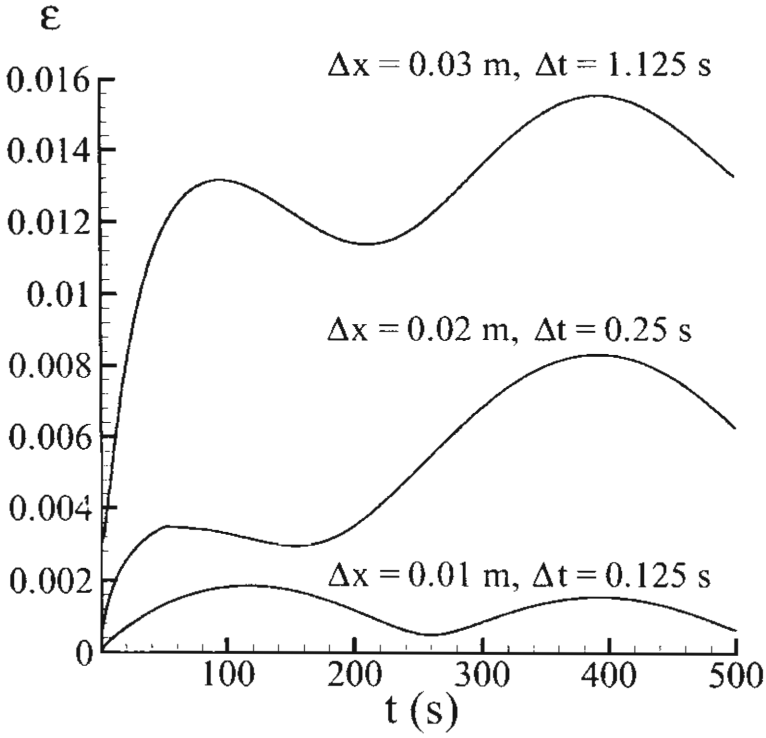
ε
0.016
0.014
0.012
0.01
0.008
0.006
0.004
0.002
0
100
200
300
400
500
t (s)
Δx = 0.03 m, Δt = 1.125 s
Δx = 0.02 m, Δt = 0.25 s
Δx = 0.01 m, Δt = 0.125 s

Figure 5

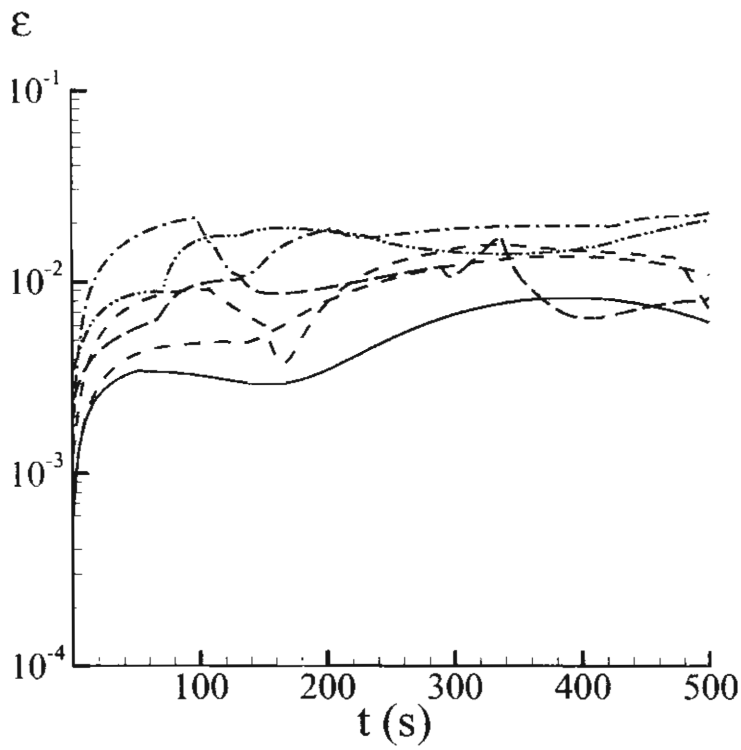

Figure 6

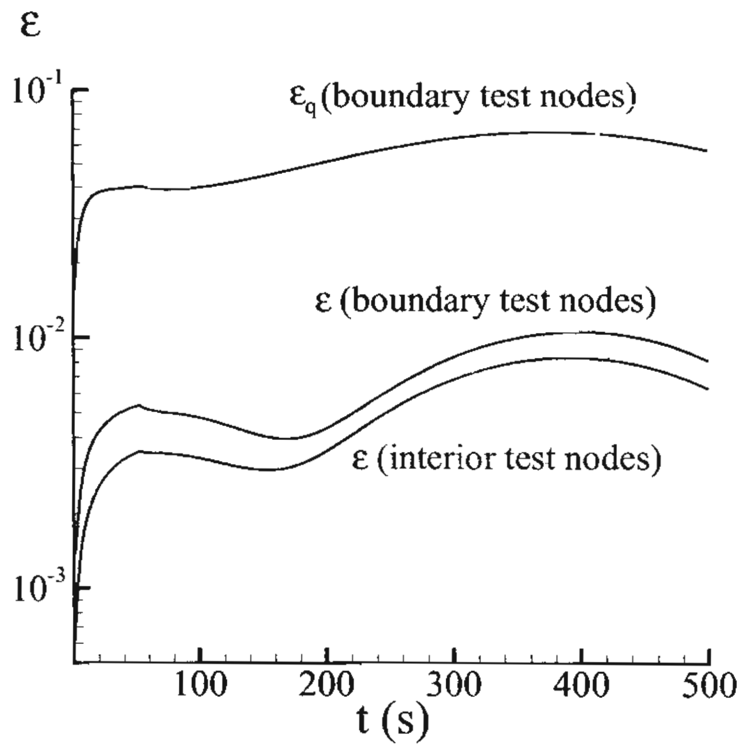
ε
10^{-1}
10^{-2}
10^{-3}
ε_q(boundary test nodes)
ε (boundary test nodes)
ε (interior test nodes)
100
200
300
400
500
t (s)

Figure 7

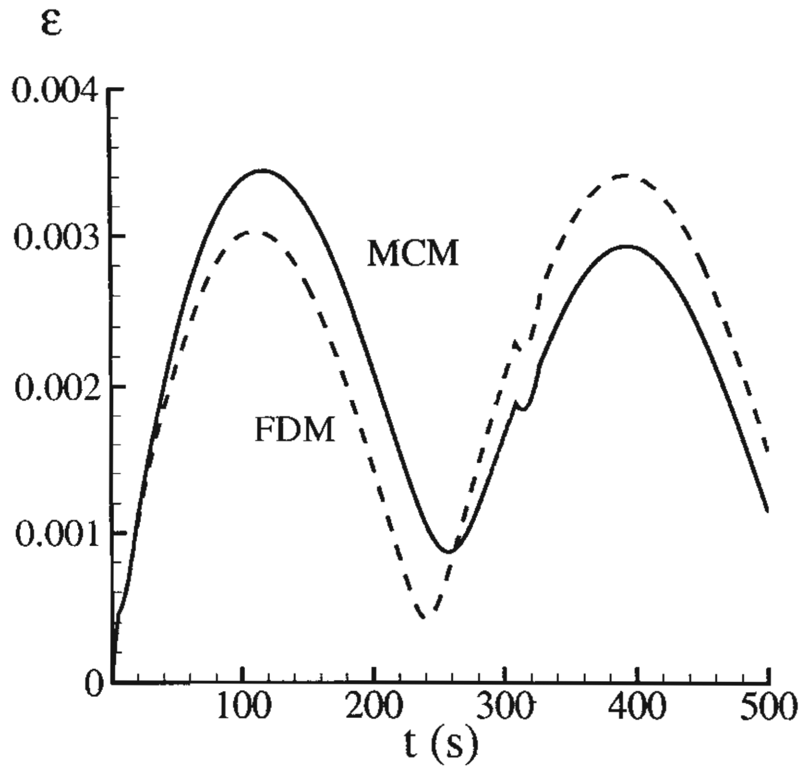

NME 1806 pp: 1-14 (col.fig.: Nil) PROD. TYPE: COM ED: Kavya PAGN: – SCAN: lakshmi

INTERNATIONAL JOURNAL FOR NUMERICAL METHODS IN ENGINEERING
Int. J. Numer. Meth. Engng (in press)
Published online in Wiley InterScience (www.interscience.wiley.com) DOI: 10.1002/nme.1806

An alternative approach for numerical solutions of the Navier–Stokes equations

S. Chantasiriwan*,†

Faculty of Engineering, Thammasat University, Rangsit Campus, Khlong Luang, Pathum Thani 12121, Thailand

SUMMARY

Conventional approaches for solving the Navier–Stokes equations of incompressible fluid dynamics are the primitive-variable approach and the vorticity–velocity approach. In this paper, an alternative approach is presented. In this approach, pressure and one of the velocity components are eliminated from the governing equations. The result is one higher-order partial differential equation with one unknown for two-dimensional problems or two higher-order partial differential equations with two unknowns for three-dimensional problems. A meshless collocation method based on radial basis functions for solving the Navier–Stokes equations using this approach is presented. The proposed method is used to solve a two- and a three-dimensional test problem of which exact solutions are known. It is found that, with appropriate values of the method parameters, solutions of satisfactory accuracy can be obtained. Copyright © 2006 John Wiley & Sons, Ltd.

Received 1 December 2005; Revised 17 May 2006; Accepted 19 May 2006

KEY WORDS: Navier–Stokes; meshless; radial basis function; multiquadrics

1. INTRODUCTION

The incompressible Navier–Stokes equations are coupled partial differential equations of pressure and velocity components. The two most popular approaches for solving these equations are the primitive-variable approach and the vorticity–velocity approach [1]. In the primitive-variable approach, the Navier–Stokes equations are to be solved for primitive variables (pressure and velocity components). The number of equations is three and four for two- and three-dimensional problems, respectively. Imposition of boundary conditions in this approach is quite straightforward. The vorticity–velocity approach requires the transformation of the Navier–Stokes equations into

*Correspondence to: S. Chantasiriwan, Faculty of Engineering, Thammasat University, Rangsit Campus, Khlong Luang, Pathum Thani 12121, Thailand.
†E-mail: somchart@engr.tu.ac.th

Contract/grant sponsor: Thailand Research Fund; contract/grant number: RSA 4680018

equations of derived variables (stream function and vorticity components). Pressure and velocity components can be easily determined once these derived variables are known. An advantage of solving the transformed equations is that there are two and three equations for two- and three-dimensional problems, respectively, which are fewer than the number of equations for corresponding problems in the primitive-variable approach. However, imposition of boundary conditions in the vorticity–velocity approach may require substantial effort, especially for three-dimensional problems, which is a major disadvantage of this strategy.

For two-dimensional problems, there is only one vorticity component, and the vorticity–velocity approach is generally known as the vorticity-stream function approach. Two equations of vorticity and stream function can be reduced to a fourth-order partial differential equation of stream function [2]. This implies that it should be possible to reduce the four Navier–Stokes equations for three-dimensional problems to two equations of two variables. Unfortunately, the vorticity–velocity approach does not allow a straightforward reduction of equations.

In this paper, an alternative approach for solving the incompressible Navier–Stokes equations is proposed. This approach reduces the number of the Navier–Stokes equations for two- and three-dimensional problems by two without requiring the transformation of the Navier–Stokes equations into equations of derived variables like the vorticity–velocity approach. The number of equations is reduced by eliminating pressure and one of the velocity components from the governing equations. As a result, there is only one equation for two-dimensional problems and two equations for three-dimensional problems. Unlike the vorticity–velocity approach, imposition of boundary conditions in the proposed approach is simple because variables to be solved for are still primitive variables. Therefore, this approach has advantages over both the primitive-variable approach and the vorticity–velocity approach. The following sections give details of this approach, a collocation method using this approach, and numerical results of using this method to solve problems with known exact solutions.

2. REDUCTION OF EQUATIONS

The two-dimensional incompressible Navier–Stokes equations are

$$u\frac{\partial u}{\partial x} + v\frac{\partial u}{\partial y} = -\frac{1}{\rho}\frac{\partial p}{\partial x} + \nu\left(\frac{\partial^2 u}{\partial x^2} + \frac{\partial^2 u}{\partial y^2}\right) \tag{1}$$

$$u\frac{\partial v}{\partial x} + v\frac{\partial v}{\partial y} = -\frac{1}{\rho}\frac{\partial p}{\partial y} + \nu\left(\frac{\partial^2 v}{\partial x^2} + \frac{\partial^2 v}{\partial y^2}\right) \tag{2}$$

$$\frac{\partial u}{\partial x} + \frac{\partial v}{\partial y} = 0 \tag{3}$$

Elimination of p from Equations (1) and (2) results in

$$u\left(\frac{\partial^2 u}{\partial x\,\partial y} - \frac{\partial^2 v}{\partial x^2}\right) + v\left(\frac{\partial^2 u}{\partial y^2} - \frac{\partial^2 v}{\partial x\,\partial y}\right) - \nu\left(\frac{\partial^3 u}{\partial x^2\,\partial y} + \frac{\partial^3 u}{\partial y^3} - \frac{\partial^3 v}{\partial x^3} - \frac{\partial^3 v}{\partial x\,\partial y^2}\right) = 0 \tag{4}$$

DOI: 10.1002/nme

Next, Equation (3) is used to express v in terms of u.

$$v=-\int \frac{\partial u}{\partial x}\,\mathrm{d}y \tag{5}$$

The incompressible three-dimensional Navier–Stokes equations are

$$u\frac{\partial u}{\partial x}+v\frac{\partial u}{\partial y}+w\frac{\partial u}{\partial z}=-\frac{1}{\rho}\frac{\partial p}{\partial x}+\nu\left(\frac{\partial^2 u}{\partial x^2}+\frac{\partial^2 u}{\partial y^2}+\frac{\partial^2 u}{\partial z^2}\right) \tag{6}$$

$$u\frac{\partial v}{\partial x}+v\frac{\partial v}{\partial y}+w\frac{\partial v}{\partial z}=-\frac{1}{\rho}\frac{\partial p}{\partial y}+\nu\left(\frac{\partial^2 v}{\partial x^2}+\frac{\partial^2 v}{\partial y^2}+\frac{\partial^2 v}{\partial z^2}\right) \tag{7}$$

$$u\frac{\partial w}{\partial x}+v\frac{\partial w}{\partial y}+w\frac{\partial w}{\partial z}=-\frac{1}{\rho}\frac{\partial p}{\partial z}+\nu\left(\frac{\partial^2 w}{\partial x^2}+\frac{\partial^2 u}{\partial y^2}+\frac{\partial^2 w}{\partial z^2}\right) \tag{8}$$

$$\frac{\partial u}{\partial x}+\frac{\partial v}{\partial y}+\frac{\partial w}{\partial z}=0 \tag{9}$$

Elimination of p from Equations (6) and (7) results in

$$u\left(\frac{\partial^2 u}{\partial x\,\partial y}-\frac{\partial^2 v}{\partial x^2}\right)+v\left(\frac{\partial^2 u}{\partial y^2}-\frac{\partial^2 v}{\partial x\,\partial y}\right)+w\left(\frac{\partial^2 u}{\partial y\,\partial z}-\frac{\partial^2 v}{\partial x\,\partial z}\right)+\frac{\partial u}{\partial y}\frac{\partial u}{\partial x}+\frac{\partial v}{\partial y}\frac{\partial u}{\partial y}+\frac{\partial w}{\partial y}\frac{\partial u}{\partial z}$$
$$-\frac{\partial u}{\partial x}\frac{\partial v}{\partial x}-\frac{\partial v}{\partial x}\frac{\partial v}{\partial y}-\frac{\partial w}{\partial x}\frac{\partial v}{\partial z}-\nu\left(\frac{\partial^3 u}{\partial x^2\,\partial y}+\frac{\partial^3 u}{\partial y^3}+\frac{\partial^3 u}{\partial y\,\partial z^2}-\frac{\partial^3 v}{\partial x^3}-\frac{\partial^3 v}{\partial x\,\partial y^2}-\frac{\partial^3 v}{\partial x\,\partial z^2}\right)=0 \tag{10}$$

Elimination of p from Equations (7) and (8) results in

$$u\left(\frac{\partial^2 v}{\partial x\,\partial z}-\frac{\partial^2 w}{\partial x\,\partial y}\right)+v\left(\frac{\partial^2 v}{\partial y\,\partial z}-\frac{\partial^2 w}{\partial y^2}\right)+w\left(\frac{\partial^2 v}{\partial z^2}-\frac{\partial^2 w}{\partial y\,\partial z}\right)+\frac{\partial u}{\partial z}\frac{\partial v}{\partial x}+\frac{\partial v}{\partial z}\frac{\partial v}{\partial y}+\frac{\partial w}{\partial z}\frac{\partial v}{\partial z}$$
$$-\frac{\partial u}{\partial y}\frac{\partial w}{\partial x}-\frac{\partial v}{\partial y}\frac{\partial w}{\partial y}-\frac{\partial w}{\partial y}\frac{\partial w}{\partial z}-\nu\left(\frac{\partial^3 v}{\partial x^2\,\partial z}+\frac{\partial^3 v}{\partial y^2\,\partial z}+\frac{\partial^3 v}{\partial z^3}-\frac{\partial^3 w}{\partial x^2\,\partial y}-\frac{\partial^3 w}{\partial y^3}-\frac{\partial^3 w}{\partial y\,\partial z^2}\right)=0 \tag{11}$$

Next, Equation (9) is used to express w in terms of u and v.

$$w=-\int\left(\frac{\partial u}{\partial x}+\frac{\partial v}{\partial y}\right)\mathrm{d}z \tag{12}$$

It can be seen that a two-dimensional problem has only one equation and one unknown (u), and a three-dimensional problem has only two equations and two unknowns (u and v). As an

DOI: 10.1002/nme

expense, the highest differential order of the reduced Navier–Stokes equations increases by one. Appropriate methods for solving these equations are collocation methods.

3. BASIS FUNCTIONS

In order to solve Equation (4) for two-dimensional problems or Equations (10) and (11) for three-dimensional problems, velocity components are expressed as linear combinations of basis functions. Let there be N collocation points. For two-dimensional problems, if the velocity component u is approximated by

$$u(x, y) = \sum_{j=1}^{N} a_j \phi(x, y, x_j, y_j) \tag{13}$$

the approximation for the velocity component v can be obtained from Equation (5):

$$v(x, y) = \sum_{j=1}^{N} a_j \psi(x, y, x_j, y_j) \tag{14}$$

where

$$\psi(x, y, x_j, y_j) = -\int \frac{\partial \phi}{\partial x}(x, y, x_j, y_j)\, \mathrm{d}y \tag{15}$$

Hence, there are only N unknown coefficients that can be determined by a collocation method. Similarly, for three-dimensional problems, if the velocity components u and v are approximated by

$$u(x, y, z) = \sum_{j=1}^{N} b_j \phi(x, y, z, x_j, y_j, z_j) \tag{16}$$

$$v(z, y, z) = \sum_{j=1}^{N} c_j \phi(x, y, z, x_j, y_j, z_j) \tag{17}$$

the approximation for the velocity component w can be obtained from Equation (12):

$$w(x, y, z) = \sum_{j=1}^{N} b_j \chi(x, y, z, x_j, y_j, z_j) + \sum_{j=1}^{N} c_j \zeta(x, y, z, x_j, y_j, z_j) \tag{18}$$

where

$$\chi(x, y, z, x_j, y_j, z_j) = -\int \frac{\partial \phi}{\partial x}(x, y, z, x_j, y_j, z_j)\, \mathrm{d}z \tag{19}$$

$$\zeta(x, y, z, x_j, y_j, z_j) = -\int \frac{\partial \phi}{\partial y}(x, y, z, x_j, y_j, z_j)\, \mathrm{d}z \tag{20}$$

Hence, there are only $2N$ unknown coefficients that can be determined by a collocation method.

In order to generate N linearly independent basis functions in Equations (13), (16) and (17), it is convenient to use radial basis functions. A radial basis function is a function that depends on the distance between the point where the function is to be evaluated and a reference point. Radial basis functions have been used for interpolating multivariate data and solving partial differential equations. Radial basis functions that are suitable for solving higher-order partial differential equations like Equations (4), (10) and (11) should be infinitely differentiable. The most commonly used radial basis functions are

Multiquadrics: $\phi(r)=\sqrt{r^2+c^2}$
Thin-plate splines: $\phi(r)=r^2\ln(r)$
Gaussians: $\phi(r)=\exp(-cr^2)$
Inverse multiquadrics: $\phi(r)=\dfrac{1}{\sqrt{r^2+c^2}}$

In addition, there is a special class of radial basis functions known as fundamental solutions, which satisfy homogeneous differential equations of certain types [3,4]. Unfortunately, such fundamental solutions are not known for most non-linear differential equations including the Navier–Stokes equations.

4. COLLOCATION METHOD

In recent decades, different collocation methods based on radial basis functions have been developed. Examples of these methods are the Kansa method [5], the method of fundamental solutions [6], the boundary knot method [7], the boundary particle method [8], etc. The Kansa method [5] has successfully been tested with a variety of linear and non-linear partial differential equations [9–14]. The collocation method used in this study is a variation of the Kansa method. Previously, the two-dimensional Navier–Stokes equations have been solved in the vorticity–velocity approach [15, 16] by collocation methods that use radial basis functions. As mentioned earlier, the development of the vorticity–velocity approach to solve the three-dimensional Navier–Stokes equations is not quite straightforward. Therefore, the primitive-variable approach has been resorted to in order to solve the three-dimensional Navier–Stokes equations by a collocation method [17]. In this section, the collocation method for solving the two- and three-dimensional Navier–Stokes equations in the proposed alternative approach is described. The collocation method is known as the multiquadric collocation method with additional collocation at the boundary. This method was used by Chantasiriwan to solve linear partial differential equations [18], and found to give more accurate solutions than the standard multiquadric collocation method that was used by Kansa [5].

4.1. Two-dimensional problem

Assume that there are N collocation nodes, divided into N_i interior nodes (indexed by $i=1,2,\ldots,N_i$) and N_b boundary nodes (indexed by $i=N_i+1,N_i+2,\ldots,N$). The velocity components u, v and their derivatives at the kth iteration are approximated as

$$u^{(k)}(x,y)=\sum_{j=1}^{N}a_j^{(k)}\phi(x,y,x_j,y_j,c)+\sum_{j=1}^{N_b}a_{j+N}^{(k)}\phi(x,y,x_{j+N_i},y_{j+N_i},d) \tag{21}$$

DOI: 10.1002/nme

$$\frac{\partial^{l+m}u^{(k)}}{\partial x^l\,\partial y^m}(x,y)=\sum_{j=1}^{N}a_j^{(k)}\frac{\partial^{l+m}\phi}{\partial x^l\,\partial y^m}(x,y,x_j,y_j,c)$$

$$+\sum_{j=1}^{N_b}a_{j+N}^{(k)}\frac{\partial^{l+m}\phi}{\partial x^l\,\partial y^m}(x,y,x_{j+N_i},y_{j+N_i},d) \tag{22}$$

$$v^{(k)}(x,y)=\sum_{j=1}^{N}a_j^{(k)}\psi(x,y,x_j,y_j,c)+\sum_{j=1}^{N_b}a_{j+N}^{(k)}\psi(x,y,x_{j-N_i},y_{j+N_i},d) \tag{23}$$

$$\frac{\partial^{l+m}v^{(k)}}{\partial x^l\,\partial y^m}(x,y)=\sum_{j=1}^{N}a_j^{(k)}\frac{\partial^{l+m}\psi}{\partial x^l\,\partial y^m}(x,y,x_j,y_j,c)$$

$$+\sum_{j=1}^{N_b}a_{j+N}^{(k)}\frac{\partial^{l+m}\psi}{\partial x^l\,\partial y^m}(x,y,x_{j-N_i},y_{j+N_i},d) \tag{24}$$

where

$$\phi(x,y,x_j,y_j,c)=\sqrt{(x-x_j)^2+(y-y_j)^2+c^2} \tag{25}$$

$$\psi(x,y,x_j,y_j,c)=-(x-x_j)\ln[2\phi(x,y,x_j,y_j,c)+2(y-y_j)] \tag{26}$$

and $c\neq d$. For the purpose of iterative determination of $N+N_b$ unknown coefficients $a_j^{(k)}$, non-linear terms in Equation (4) are linearized by the scheme proposed by Ferziger and Peric [19]. For example,

$$u^{(k)}\frac{\partial^2u^{(k)}}{\partial x\,\partial y}=u^{(k-1)}\frac{\partial^2u^{(k)}}{\partial x\,\partial y}+u^{(k)}\frac{\partial^2u^{(k-1)}}{\partial x\,\partial y}-u^{(k-1)}\frac{\partial^2u^{(k-1)}}{\partial x\,\partial y} \tag{27}$$

After linearization, Equation (4) represents N equations for $(x,y)=(x_i,y_i)$ $(i=1,2,\ldots,N)$. Boundary conditions for u and v yield $2N_b$ more equations. Therefore, the resulting system of equations can be solved by a least-square method because there are more equations than unknowns. Initially, let $a_j^{(0)}=0$. The iteration process is continued until the convergence criterion are satisfied:

$$\sqrt{\frac{1}{N_i}\sum_{i=1}^{N_i}\left(1-\frac{f_i^{(k-1)}}{f_i^{(k)}}\right)^2}<10^{-5} \tag{28}$$

where f represents a velocity component.

4.2. Three-dimensional problem

The velocity components u, v, w and their derivatives at the kth iteration are approximated as

$$u^{(k)}(x,y,z)=\sum_{j=1}^{N}a_j^{(k)}\phi(x,y,z,x_j,y_j,z_j,c)$$

DOI: 10.1002/nme

$$+\sum_{j=1}^{N_b} a_{j+N}^{(k)}\phi(x,y,z,x_{j+N_i},y_{j+N_i},z_{j+N_i},d) \tag{29}$$

$$\frac{\partial^{l+m+n}u^{(k)}}{\partial x^l\,\partial y^m\,\partial z^n}(x,y,z)=\sum_{j=1}^{N} a_j^{(k)}\frac{\partial^{l+m+n}\phi}{\partial x^l\,\partial y^m\,\partial z^n}(x,y,z,x_j,y_j,z_j,c)$$

$$+\sum_{j=1}^{N_b} a_{j+N}^{(k)}\frac{\partial^{l+m+n}\phi}{\partial x^l\,\partial y^m\,\partial z^n}(x,y,z,x_{j+N_i},y_{j+N_i},z_{j+N_i},d) \tag{30}$$

$$v^{(k)}(x,y,z)=\sum_{j=1}^{N} b_j^{(k)}\phi(x,y,z,x_j,y_j,z_j,c)$$

$$+\sum_{j=1}^{N_b} b_{j+N}^{(k)}\phi(x,y,z,x_{j+N_i},y_{j+N_i},z_{j+N_i},d) \tag{31}$$

$$\frac{\partial^{l+m+n}v^{(k)}}{\partial x^l\,\partial y^m\,\partial z^n}(x,y,z)=\sum_{j=1}^{N} b_j^{(k)}\frac{\partial^{l+m+n}\phi}{\partial x^l\,\partial y^m\,\partial z^n}(x,y,z,x_j,y_j,z_j,c)$$

$$+\sum_{j=1}^{N_b} b_{j+N}^{(k)}\frac{\partial^{l+m+n}\phi}{\partial x^l\,\partial y^m\,\partial z^n}(x,y,z,x_{j+N_i},y_{j+N_i},z_{j+N_i},d) \tag{32}$$

$$w^{(k)}(x,y,z)=\sum_{j=1}^{N} a_j^{(k)}\chi(x,y,z,x_j,y_j,z_j,c)$$

$$+\sum_{j=1}^{N_b} a_{j+N}^{(k)}\chi(x,y,z,x_{j+N_i},y_{j+N_i},z_{j+N_i},d)$$

$$+\sum_{j=1}^{N} b_j^{(k)}\zeta(x,y,z,x_j,y_j,z_j,c)$$

$$+\sum_{j=1}^{N_b} b_{j+N}^{(k)}\zeta(x,y,z,x_{j+N_i},y_{j+N_i},z_{j+N_i},d) \tag{33}$$

$$\frac{\partial^{l+m+n}w^{(k)}}{\partial x^l\,\partial y^m\,\partial z^n}(x,y,z)=\sum_{j=1}^{N} a_j^{(k)}\frac{\partial^{l+m+n}\chi}{\partial x^l\,\partial y^m\,\partial z^n}(x,y,z,x_j,y_j,z_j,c)$$

$$+\sum_{j=1}^{N_b} a_{j+N}^{(k)}\frac{\partial^{l+m+n}\chi}{\partial x^l\,\partial y^m\,\partial z^n}(x,y,z,x_{j+N_i},y_{j+N_i},z_{j+N_i},d)$$

DOI: 10.1002/nme

$$+\sum_{j=1}^{N} b_j^{(k)} \frac{\partial^{l+m+n}\zeta}{\partial x^l\,\partial y^m\,\partial z^n}(x, y, z, x_j, y_j, z_j, c)$$

$$+\sum_{j=1}^{N_b} b_{j+N}^{(k)} \frac{\partial^{l+m+n}\zeta}{\partial x^l\,\partial y^m\,\partial z^n}(x, y, z, x_{j+N_i}, y_{j+N_i}, z_{j+N_i}, d) \tag{34}$$

where

$$\phi(x, y, z, x_j, y_j, z_j, c) = \sqrt{(x - x_j)^2 + (y - y_j)^2 + (z - z_j)^2 + c^2} \tag{35}$$

$$\chi(x, y, z, x_j, y_j, z_j, c) = -(x - x_j)\ln[2\phi(x, y, z, x_j, y_j, z_j, c) + 2(z - z_j)] \tag{36}$$

$$\zeta(x, y, z, x_j, y_j, z_j, c) = -(y - y_j)\ln[2\phi(x, y, z, x_j, y_j, z_j, c) + 2(z - z_j)] \tag{37}$$

and $c \neq d$. For the purpose of iterative determination of $2(N + N_b)$ unknown coefficients $a_j^{(k)}$ and $b_j^{(k)}$, non-linear terms in Equations (10) and (11) are linearized by a scheme proposed by Ferziger and Peric [19]. After linearization, Equations (10) and (11) represent $2N$ equations for $(x, y, z) = (x_i, y_i, z_i)$ $(i = 1, 2, \ldots, N)$. Boundary conditions for u, v and w yield $3N_b$ more equations. Therefore, the resulting system of equations can be solved by a least-square method because there are more equations than unknowns. Initially, let $a_j^{(0)} = b_j^{(0)} = 0$. The iteration process is continued until the convergence criterion (Equation (28)) is satisfied.

5. RESULTS AND DISCUSSION

Two test problems having Dirichlet boundary conditions are considered. Let (ξ_i, η_i) be co-ordinates of a test node in the two-dimensional test problem and $(\xi_i, \eta_i, \gamma_i)$ be co-ordinates of a test node in the three-dimensional test problem. Velocity components at the test node can be calculated from Equations (13) and (14) or Equations (16)–(18) after coefficients have been determined. If the exact solutions are known, errors can be computed from

$$\varepsilon_f = \sqrt{\frac{\sum_{i=1}^{N_t} [f_{\text{numer}}(\xi_i, \eta_i) - f_{\text{exact}}(\xi_i, \eta_i)]^2}{\sum_{i=1}^{N_t} [f_{\text{exact}}(\xi_i, \eta_i)]^2}} \tag{38}$$

or

$$\varepsilon_f = \sqrt{\frac{\sum_{i=1}^{N_t} [f_{\text{numer}}(\xi_i, \eta_i, \gamma_i) - f_{\text{exact}}(\xi_i, \eta_i, \gamma_i)]^2}{\sum_{i=1}^{N_t} [f_{\text{exact}}(\xi_i, \eta_i, \gamma_i)]^2}} \tag{39}$$

where N_t is the number of test nodes, and f represents velocity component u, v or w.

DOI: 10.1002/nme

5.1. Two-dimensional test problem

The domain for the two-dimensional test problem is a 1×1 square. There are 64 test nodes located at $(\frac{i}{8}+\frac{1}{16}, \frac{j}{8}+\frac{1}{16})$ with integers i and j running from -4 to 3. N collocation nodes are uniformly distributed in the domain, forming a square grid. Exact solutions for this problem are

$$u_{\text{exact}}(x, y) = e^{\lambda(x+y)} + \lambda y \tag{40}$$

$$v_{\text{exact}}(x, y) = -e^{\lambda(x-y)} + \lambda y \tag{41}$$

From these exact solutions, boundary conditions are generated, and numerical solutions are determined by the proposed method. In the following results, it is shown how ε_u and ε_v vary with the shape parameters (c and d) and other parameters.

Figure 1 shows influences of the shape parameters c and d on ε_u and ε_v for the case in which $\lambda = -1$, $v = 1$, and $N = 81$. Solutions are more accurate as c is increased. When c is too large, however, it is found that no converged solution can be found. A large value of c is associated with high condition number of the coefficient matrix of the system of linear equations. Since the computing machine used in this study has a limited precision, an ill-conditioned system of linear equations cannot be solved with high precision. This may be a reason why the proposed method does not converge when a certain value of c is reached. In addition, Figure 1 also shows that solutions are relatively insensitive to the shape parameter d between $c+0.1$ and $c+0.2$.

Figure 2 compares ε_u and ε_v of solutions for three values of N (49, 81, 121) with $\lambda = -1$ and $v = 1$. The shape parameter d is varied with N so that the difference between d and c scales with grid spacing. The range of the shape parameter c in which a converged solution can be obtained is narrower as N is increased. An interesting consequence of this is that solutions with a larger

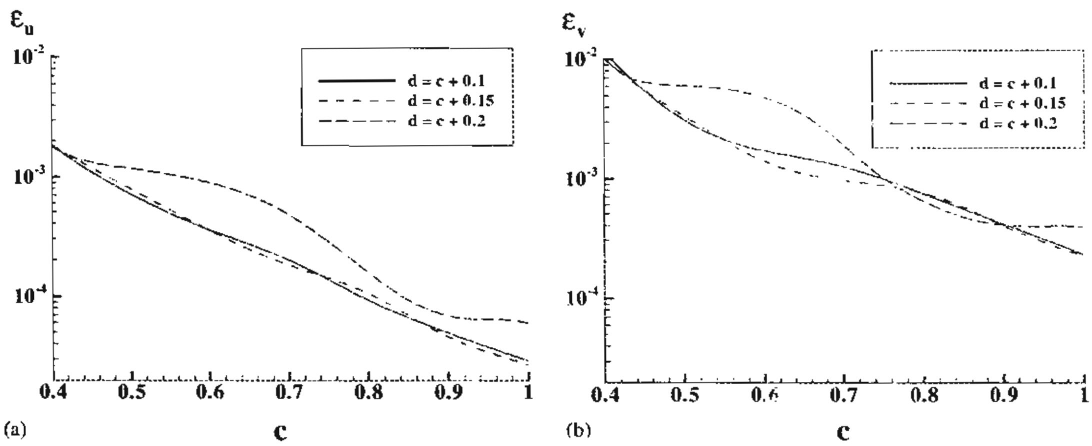

Figure 1. Variations of errors of velocity components (ε_u and ε_v) with the shape parameters c and d for the two-dimensional test problem having parameters $\lambda = -1$ and $v = 1$. The number of collocation nodes (N) is 81.

DOI: 10.1002/nme

NME 1806

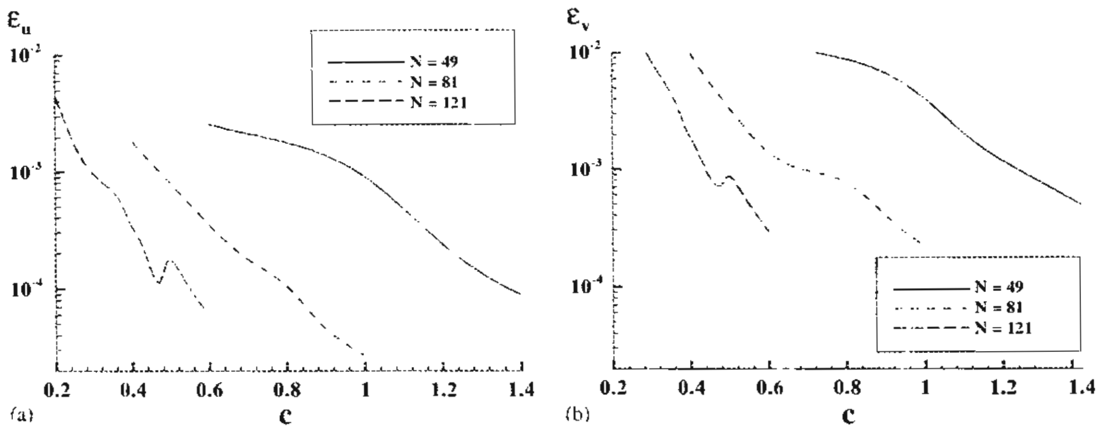

Figure 2. Variations of errors of velocity components (ε_u and ε_v) with the shape parameters c and the number of collocation nodes (N) for the two-dimensional test problem having parameters $\lambda = -1$ and $v = 1$. The shape parameter d equals $c + 0.2$ for $N = 49$, $c + 0.15$ for $N = 81$, and $c + 0.12$ for $N = 121$.

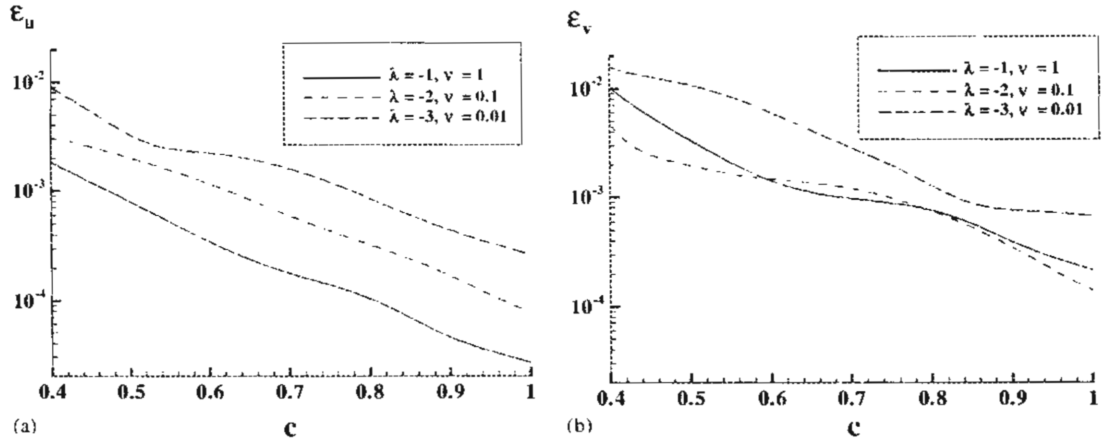

Figure 3. Variations of errors of velocity components (ε_u and ε_v) with the shape parameter c for the two-dimensional test problem having three sets of parameters: $(\lambda, v) = (-1, 1)$, $(-2, 0.1)$, and $(-3, 0.01)$. The number of collocation nodes (N) is 81, and the shape parameter $d = c + 0.15$.

number of nodes and smaller values of shape parameters may not be more accurate than solutions with a smaller number of nodes and larger values of shape parameters.

The proposed method is also tested with cases in which λ and v are smaller than -1 and 1, respectively. These cases present a stiffer challenge because their exact solutions are less smooth than the exact solution for which $\lambda = -1$, $v = 1$. It can be seen from Figure 3 that the proposed method can solve the test problem in which $(\lambda, v) = (-2, 0.1)$ and $(-3, 0.01)$. It is found, however, the method requires more iterations to converge and the converged solution is less accurate as λ and v become smaller.

DOI: 10.1002/nme

NME 1806

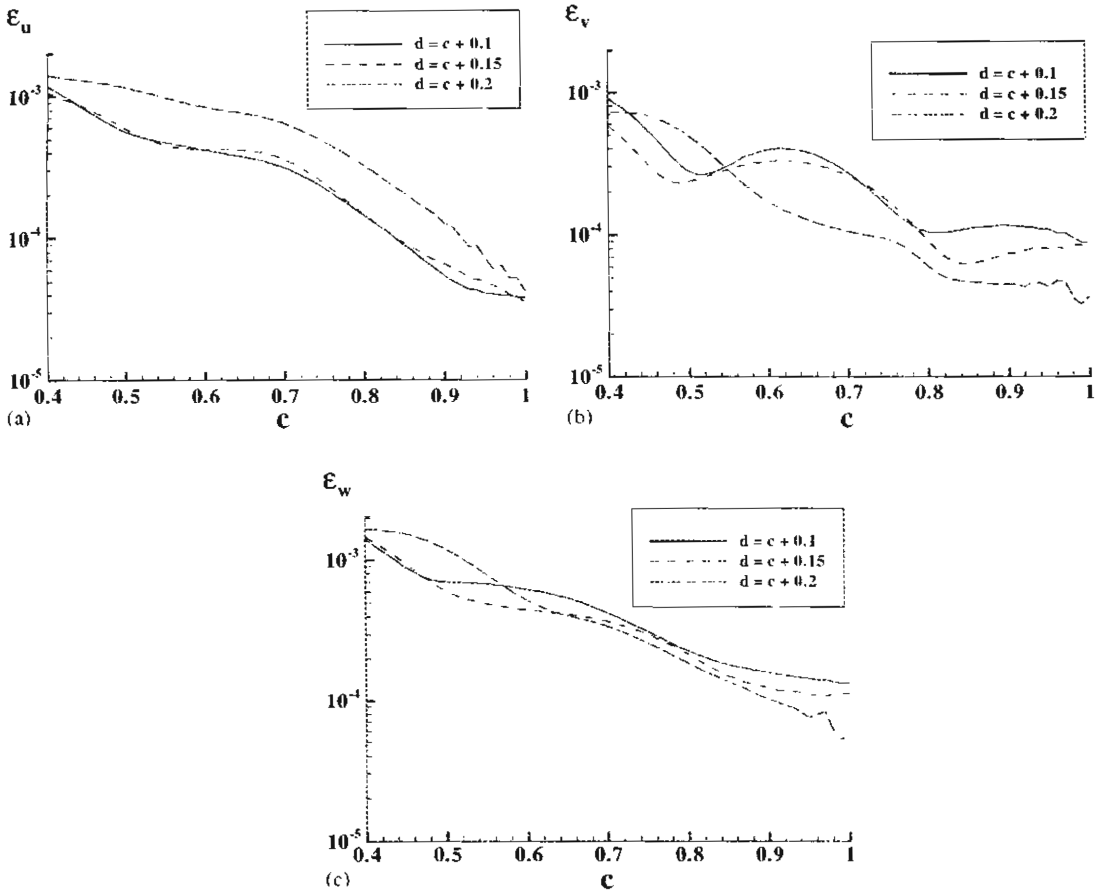

Figure 4. Variations of errors of velocity components (ε_u, ε_v, and ε_w) with the shape parameters c and d for the three-dimensional test problem having parameters $\lambda = -1$ and $v = 1$. The number of collocation nodes (N) is 729.

5.2. *Three-dimensional test problem*

The domain for the three-dimensional test problem is a $1 \times 1 \times 1$ cube. There are 512 test nodes located at $(\frac{i}{8} + \frac{1}{16}, \frac{j}{8} + \frac{1}{16}, \frac{k}{8} + \frac{1}{16})$ with integers i, j and k running from -4 to 3. N collocation nodes are uniformly distributed in the domain, forming a cube grid. Exact solutions for this problem are

$$u_{\text{exact}}(x, y, z) = 2e^{\lambda(x+y+z)} + \lambda v \tag{42}$$

$$v_{\text{exact}}(x, y, z) = -e^{\lambda(x+y+z)} + \lambda v \tag{43}$$

$$w_{\text{exact}}(x, y, z) = -e^{\lambda(x+y+z)} + \lambda v \tag{44}$$

DOI: 10.1002/nme

NME 1806

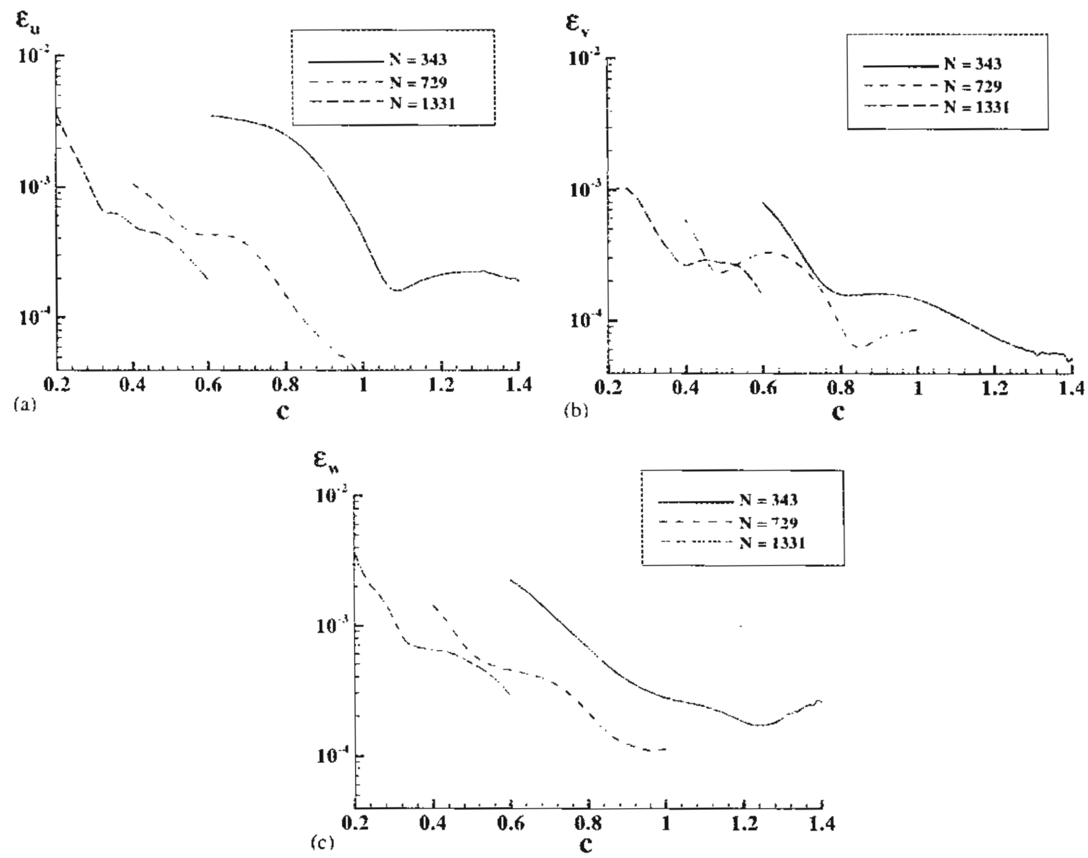

Figure 5. Variations of errors of velocity components (ε_u, ε_v, and ε_w) with the shape parameters c and the number of collocation nodes (N) for the two-dimensional test problem having parameters $\lambda = -1$ and $v = 1$. The shape parameter d equals $c + 0.2$ for $N = 343$, $c + 0.15$ for $N = 729$, and $c + 0.12$ for $N = 1331$.

From these exact solutions, boundary conditions are generated, and numerical solutions are determined by using the proposed method. In the following results, it is shown how ε_u, ε_v and ε_w vary with the shape parameter c and other parameters.

Results for the three-dimensional test problem are similar to those for the two-dimensional test problem. Figure 4 shows that a larger value of the shape parameter c leads to more accurate solutions, but the method may not converge if c is too large. Figure 5 compares errors of solutions obtained with $N = 343, 729$, and 1331. It can be seen that the range of the shape parameter c for which the proposed method converges is narrower as N is increased. Figure 6 compares errors of solutions for which $(\lambda, v) = (-1, 1), (-2, 0.1)$ and $(-3, 0.01)$. The method is more difficult to converge, and the converged solution is less accurate as λ and v become smaller.

DOI: 10.1002/nme

NME 1806

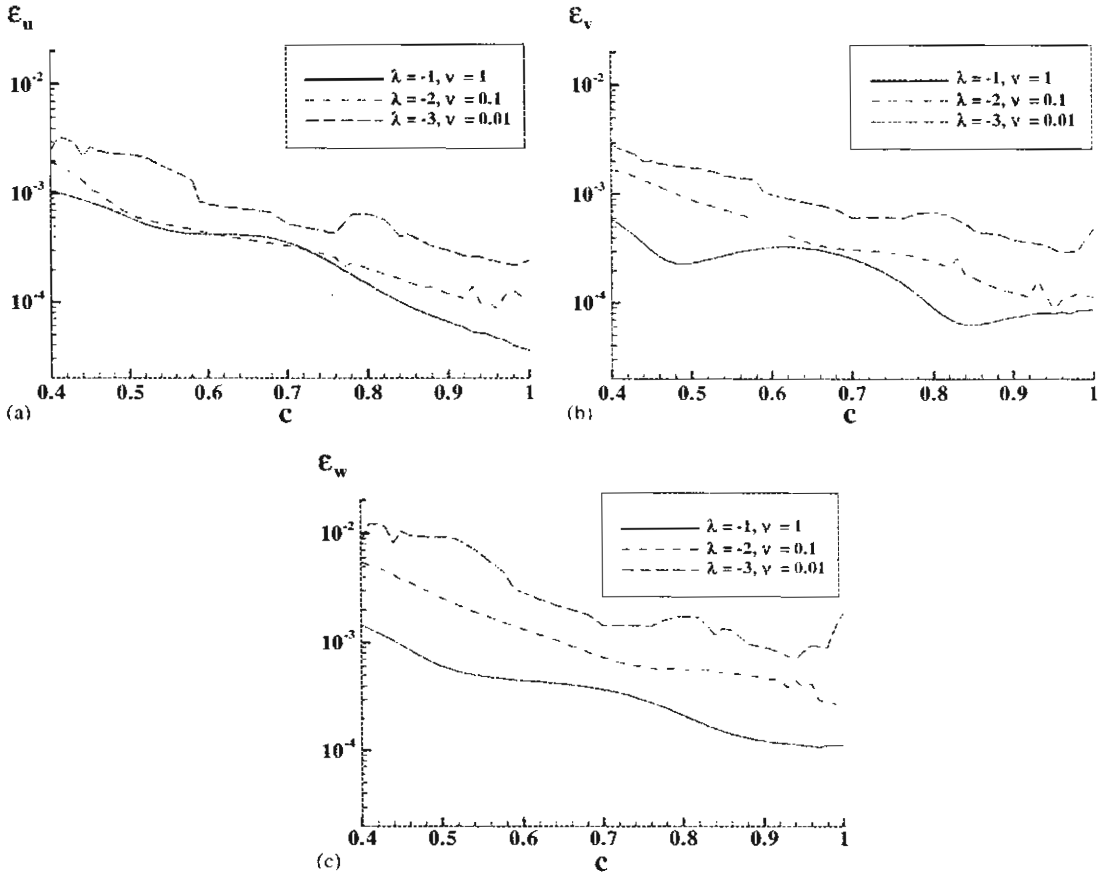

Figure 6. Variations of errors of velocity components (ε_u, ε_v, and ε_w) with the shape parameter c for the three-dimensional test problem having three sets of parameters: $(\lambda, v) = (-1, 1), (-2, 0.1)$, and $(-3, 0.01)$. The number of collocation nodes (N) is 729, and the shape parameter $d = c + 0.15$.

6. CONCLUSIONS

This paper presents an alternative approach for solving the Navier–Stokes equations, in which pressure and one of the velocity components are eliminated, and the governing equations are reduced to higher-order partial differential equations of the remaining velocity components. The resulting equations are solved by a meshless collocation method that uses multiquadrics and associated functions as basis functions. Inspection of solutions to two test problems by the proposed method reveals that shape parameters of multiquadrics influence the accuracy of solutions. There appears to be an upper limit to values of shape parameters for which the method is capable of providing a converged solution. This limit decreases as the number of collocation nodes increases.

ACKNOWLEDGEMENTS

The author would like to acknowledge the financial support from the Thailand Research Fund.

NME 1806

REFERENCES

1. Tanhill JC, Anderson DA, Pletcher RH. *Computational Fluid Mechanics and Heat Transfer* (2nd edn). Taylor and Francis: Washington, DC, 1997; 649–677.
2. Polyanin AD, Zaitsev VF. *Handbook of Nonlinear Partial Differential Equations*. Chapman and Hall/CRC Press: Boca Raton, 2003; 607.
3. Golberg MA. Method of fundamental solutions for Poisson's equation. *Engineering Analysis with Boundary Elements* 1995; **16**(3):205–213.
4. Chen W, Shen LJ, Shen ZJ, Yuan GW. Boundary knot method for Poisson equations. *Engineering Analysis with Boundary Elements* 2005; **29**(8):756–760.
5. Kansa EJ. Multiquadrics—A scattered data approximation scheme with applications to computational fluid-dynamics—II solutions to parabolic, hyperbolic and elliptic partial differential equations. *Computers and Mathematics with Applications* 1990; **19**(8–9):147–161.
6. Fairweather G, Karageorghis A. The method of fundamental solutions for elliptic boundary value problems. *Advances in Computational Mathematics* 1998; **9**(1–2):69–95.
7. Chen W, Tanaka M. A meshless, integration-free, and boundary-only RBF technique. *Computers and Mathematics with Applications* 2002; **43**(3–5):379–391.
8. Chen W. Meshfree boundary particle method applied to Helmholtz problems. *Engineering Analysis with Boundary Elements* 2002; **26**(7):577–581.
9. Zerroukat M, Power H, Chen CS. A numerical method for heat transfer problems using collocation and radial basis functions. *International Journal for Numerical Methods in Engineering* 1998; **42**(7):1263–1278.
10. Hon YC, Mao XZ. An efficient numerical scheme for Burgers' equation. *Applied Mathematics and Computation* 1998; **95**(1):37–50.
11. Fedoseyev AI, Friedman MJ, Kansa EJ. Continuation for nonlinear elliptic partial differential equations discretized by the multiquadric method. *International Journal of Bifurcation and Chaos in Applied Sciences and Engineering* 2000; **10**(2):481–492.
12. Li J, Chen CS. Some observations on unsymmetric radial basis function collocation methods for convection–diffusion problems. *International Journal for Numerical Methods in Engineering* 2003; **57**(8):1085–1094.
13. Zhoua X, Hon YC, Cheung KF. A grid-free, nonlinear shallow-water model with moving boundary. *Engineering Analysis with Boundary Elements* 2004; **28**(8):967–973.
14. Young DL, Jane SC, Lin CY, Chiu CL, Chen KC. Solutions of 2D and 3D Stokes laws using multiquadrics method. *Engineering Analysis with Boundary Elements* 2004; **28**(10):1233–1243.
15. Mai-Duy M, Tran-Cong T. Numerical solution of Navier–Stokes equations using multiquadric radial basis function networks. *International Journal for Numerical Methods in Fluids* 2001; **37**(1):65–86.
16. Shu C, Ding H, Yeo KS. Computation of incompressible Navier–Stokes equations by local RBF-based differential quadrature method. *CMES—Computer Modeling in Engineering and Sciences* 2005; **7**(2):195–205.
17. Ding H, Shu C, Yeo KS, Xu D. Numerical computation of three-dimensional incompressible viscous flows in the primitive variable form by local multiquadric differential quadrature method. *Computer Methods in Applied Mechanics and Engineering* 2006; **195**(7–8):516–533.
18. Chantasiriwan S. Cartesian grid methods using radial basis functions for solving Poisson, Helmholtz, and diffusion–convection equations. *Engineering Analysis with Boundary Elements* 2004; **28**(12):1417–1425.
19. Ferziger JH, Milovan P. *Computational Methods for Fluid Dynamics*. Springer: Berlin, 1997; 115.

DOI: 10.1002/nme

cnme@cfdlab.ae.utexas.edu
Communications in Numerical Methods in Engineering - Decision on Manuscript # CNM-Aug-05-0091.R1
Mon, 8 พฤษภาคม,2006 10:58 pm
somchart@engr.tu.ac.th

06

:hantasiriwan

ı for sending the marked copy of your revised manuscript entitled
ɔn Methods Based on Radial Basis Functions for Solving Stochastic Poisson
' to the journal Communications in Numerical Methods in Engineering. It is a
:o accept your manuscript in its current form for publication.

copyright transfer agreement is needed for publication. Please can you
s the copyright transfer agreement at
w3.interscience.wiley.com/cgi-bin/jabout/5902/ForAuthors.html or download
ıed copyright transfer agreement. Please complete the necessary fields,
ı it to the publisher as soon as possible at the following address.

resolve custom email tag

ry important as the publishing process cannot commence until the agreement
received. Please ensure that the agreement is identified with the
number given above.

u for your contribution.

ıam F Carey
ɔmmunications in Numerical Methods in Engineering
dlab.ae.utexas.edu

===
lable online, all articles from Communications in Numerical Methods in
ing since 1985, Volume 1, Issue 1. More information at
w3.interscience.wiley.com/cgi-bin/collectionhome/NMCOL/HOME

lable online, the Encyclopedia of Computational
s: http://www3.interscience.wiley.com/cgi-bin/mrwhome/109862874/HOME

clopedia also exists in print:
.wiley.com/WileyCDA/WileyTitle/productCd-0470846992.html
===

ดาวน์โหลดจดหมายนี้

ahs@mae.uta.edu
AE Recommendation on Paper HT-05-1166 (Research Paper)
Thu, 20 เมษายน,2006 2:37 am
somchart@engr.tu.ac.th
ahs@mae.uta.edu,jaluria@jove.rutgers.edu,spatel@jove.rutgers.edu

:ar Somchart Chantasiriwan,

:view has been completed on your paper, HT-05-1166 (Research Paper), Multiquadric
ion Method for Time-dependent Heat Conduction Problems with
ature-dependent Thermal Properties.

n the detailed comments of the reviewers, I am recommending to the Journal
hat your paper be accepted for publication as a Research Paper in the
of Heat Transfer. My recommendation is:
ble: Minor changes only.

ailed comments of the reviewers are available for your further consideration.
og in to the web site to see these comments.

ommendation is also being forwarded to the Journal Editor, who will notify
he final decision and the next steps necessary in the publication process.

ontact me with any further questions.

ou.

cerely,
Haji-Sheikh
sociate Editor, Journal of Heat Transfer

ดาวน์โหลดจดหมายนี้

ijnme-us@northwestern.edu
NME-Dec-05-0643.R2 - Decision
Sat, 20 พฤษภาคม,2006 2:39 am
somchart@engr.tu.ac.th

---

tasiriwan,

e to accept your manuscript entitled "An Alternative Approach for
utions of the Navier-Stokes Equations" in its current form for
the International Journal for Numerical Methods in Engineering.

right transfer agreement is needed for publication. Please can you
pyright transfer agreement at
nterscience.wiley.com/cgi-bin/jabout/1430/ForAuthors.html or download
copyright transfer agreement. Please complete the necessary fields and
e publisher as soon as possible at the following address

ore
Sons, Ltd

:

nportant as the publishing process cannot commence until the agreement
ived. Please ensure that you have identified the agreement with the
nber given above.

your contribution.

tschko
ational Journal for Numerical Methods in Engineering
@northwestern.edu

ดาวน์โหลดจดหมายนี้

III European Conference on Computational Mechanics
Solids, Structures and Coupled Problems in Engineering
C.A. Mota Soares et.al. (eds.)
Lisbon, Portugal, 5–8 June 2006

SOLUTION OF THE STATIONARY THREE-DIMENSIONAL NAVIER-STOKES EQUATIONS BY USING RADIAL BASIS FUNCTIONS AND REDUCING THE NUMBER OF GOVERNING EQUATIONS

Somchart Chantasiriwan

Faculty of Engieering, Thammasat University, Rangsit Campus
Khlong Luang, Pathum Thani 12121, Thailand
e-mail: somchart@engr.tu.ac.th

Keywords: Navier-Stokes; meshless; radial basis function; multiquadrics.

Abstract. *The stationary three-dimensional Navier-Stokes equations consisting of four equations and four unknowns have been solved by conventional methods using the primitive-variable approach. By getting rid of pressure and one of the velocity components, the Navier-Stokes equations can be reduced to two higher-order partial differential equations with the remaining two velocity components as the only unknowns. In this paper, a meshless method based on a radial basis function, known as multiquadrics, is proposed for solving such equations. Unknown velocity components are approximated as linear combinations of multiquadrics centered at domain nodes and boundary nodes. Unknown coefficients are determined by an iterative scheme. The proposed method is used to solve a test problem, for which exact solution is known. It is found that the number of iterations required for a converged solution and the accuracy of the solution depend on the shape parameter of multiquadrics. A small value of the shape parameter results in a low number of required iterations, but the resulting solution may not be accurate. On the other hand, a large value of the shape parameter can yield a very accurate solution provided that a converged solution is obtained.*

1 INTRODUCTION

The incompressible Navier-Stokes equations are coupled partial differential equations of pressure and velocity components. The two most popular approaches for solving these equations are the primitive-variable approach and the vorticity-velocity approach [1]. In the primitive-variable approach, the Navier-stokes equations are solved for primitive variables (pressure and velocity components). Imposition of boundary conditions in this approach is quite straightforward. The vorticity-velocity approach requires the transformation of the Navier-Stokes equations into equations of derived variables (vorticity components and velocity potential). Pressure and velocity components can be easily determined once these derived variables are known. An advantage of solving the transformed equations is that there are fewer equations to be solved. However, imposition of boundary conditions in the vorticity-velocity approach may require substantial effort, especially for three-dimensional problems, which is an important disadvantage of this approach.

In this paper, an alternative approach for solving the three-dimensional Navier-Stokes equations is proposed. This approach reduces the number of the Navier-Stokes equations by two without requiring the transformation of the Navier-Stokes equations into equations of derived variables like the vorticity-velocity approach. The number of equations is reduced by eliminating pressure and one of the velocity components from the governing equations. As a result, there are only two equations left. Unlike the vorticity-velocity approach, imposition of boundary conditions in the proposed approach is simple because variables to be solved for are still primitive variables. Therefore, this approach has advantages over both the primitive-variable approach and the vorticity-velocity approach. The following sections give details of this approach, a collocation method using this approach, and numerical results of using this method to solve a test problem with known exact solution.

2 REDUCTION OF EQUATIONS

The three-dimensional Navier-Stokes equations are

$$u\frac{\partial u}{\partial x}+v\frac{\partial u}{\partial y}+w\frac{\partial u}{\partial z}=-\frac{1}{\rho}\frac{\partial p}{\partial x}+\nu\left(\frac{\partial^2 u}{\partial x^2}+\frac{\partial^2 u}{\partial y^2}+\frac{\partial^2 u}{\partial z^2}\right) \tag{1}$$

$$u\frac{\partial v}{\partial x}+v\frac{\partial v}{\partial y}+w\frac{\partial v}{\partial z}=-\frac{1}{\rho}\frac{\partial p}{\partial y}+\nu\left(\frac{\partial^2 v}{\partial x^2}+\frac{\partial^2 v}{\partial y^2}+\frac{\partial^2 v}{\partial z^2}\right) \tag{2}$$

$$u\frac{\partial w}{\partial x}+v\frac{\partial w}{\partial y}+w\frac{\partial w}{\partial z}=-\frac{1}{\rho}\frac{\partial p}{\partial z}+\nu\left(\frac{\partial^2 w}{\partial x^2}+\frac{\partial^2 w}{\partial y^2}+\frac{\partial^2 w}{\partial z^2}\right) \tag{3}$$

$$\frac{\partial u}{\partial x}+\frac{\partial v}{\partial y}+\frac{\partial w}{\partial z}=0 \tag{4}$$

Elimination of p from Equations (1) and (2) results in

$$\begin{aligned}
u\left(\frac{\partial^2 u}{\partial x\partial y}-\frac{\partial^2 v}{\partial x^2}\right)+v\left(\frac{\partial^2 u}{\partial y^2}-\frac{\partial^2 v}{\partial x\partial y}\right)+w\left(\frac{\partial^2 u}{\partial y\partial z}-\frac{\partial^2 v}{\partial x\partial z}\right)+\\
\frac{\partial u}{\partial y}\frac{\partial u}{\partial x}+\frac{\partial v}{\partial y}\frac{\partial u}{\partial y}+\frac{\partial w}{\partial y}\frac{\partial u}{\partial z}-\frac{\partial u}{\partial x}\frac{\partial v}{\partial x}-\frac{\partial v}{\partial x}\frac{\partial v}{\partial y}-\frac{\partial w}{\partial x}\frac{\partial v}{\partial z}-\\
\nu\left(\frac{\partial^3 u}{\partial x^2\partial y}+\frac{\partial^3 u}{\partial y^3}+\frac{\partial^3 u}{\partial y\partial z^2}-\frac{\partial^3 v}{\partial x^3}-\frac{\partial^3 v}{\partial x\partial y^2}-\frac{\partial^3 v}{\partial x\partial z^2}\right)=0
\end{aligned} \tag{5}$$

Elimination of p from Equations (2) and (3) results in

$$u\left(\frac{\partial^2 v}{\partial x\partial z}-\frac{\partial^2 w}{\partial x\partial y}\right)+v\left(\frac{\partial^2 v}{\partial y\partial z}-\frac{\partial^2 w}{\partial y^2}\right)+w\left(\frac{\partial^2 v}{\partial z^2}-\frac{\partial^2 w}{\partial y\partial z}\right)+$$
$$\frac{\partial u}{\partial z}\frac{\partial v}{\partial x}+\frac{\partial v}{\partial z}\frac{\partial v}{\partial y}+\frac{\partial w}{\partial z}\frac{\partial v}{\partial z}-\frac{\partial u}{\partial y}\frac{\partial w}{\partial x}-\frac{\partial v}{\partial y}\frac{\partial w}{\partial y}-\frac{\partial w}{\partial y}\frac{\partial w}{\partial z}-$$
$$\nu\left(\frac{\partial^3 v}{\partial x^2\partial z}+\frac{\partial^3 v}{\partial y^2\partial z}+\frac{\partial^3 v}{\partial z^3}-\frac{\partial^3 w}{\partial x^2\partial y}-\frac{\partial^3 w}{\partial y^3}-\frac{\partial^3 w}{\partial y\partial z^2}\right)=0 \qquad (6)$$

Next, Equation (4) is used to express w in terms of u and v.

$$w = -\int\left(\frac{\partial u}{\partial x}+\frac{\partial v}{\partial y}\right)dz \qquad (7)$$

It can be seen that the problem has only two equations and two unknowns (u and v). In exchange for the reduction of the number of equations, the resulting governing equations are now higher-order nonlinear partial differential equations. An appropriate method for solving these equations is a collocation method.

3 COLLOCATION METHOD

Collocation methods based on radial basis functions were popularized by Kansa [2]. They have been used to solve a variety of linear and nonlinear partial differential equations [3, 4, 5, 6, 7, 8]. Previously, the two-dimensional Navier-Stokes equations have been solved in the vorticity-velocity approach [9, 10] by collocation methods that use radial basis functions. As mentioned earlier, the development of the vorticity-velocity approach to solve the three-dimensional Navier-Stokes equations is not quite straightforward. Therefore, the primitive-variable approach has been resorted to in order to solve the three-dimensional Navier-Stokes equations by a collocation method [11]. In this section, the collocation method for solving the three-dimensional Navier-Stokes equations is described. The collocation method is known as the multiquadric collocation method with additional collocation at the boundary. This method was used by Chantasiriwan to solve linear partial differential equations [12], and found to give more accurate solutions than the standard multiquadric collocation method that was used by Kansa [2].

Assume that there are N nodes, divided into N_b boundary nodes (indexed by $i = 1, 2, ..., N_b$) and N_i interior nodes (indexed by $i = N_b+1, N_b+2, ..., N$). The first derivatives of the velocity components u and v at the k$^{\text{th}}$ iteration are approximated as

$$\frac{\partial u^{(k)}}{\partial x}=\sum_{j=1}^{N}a_j^{(k)}\phi(x,y,z,x_j,y_j,z_j,c)+\sum_{j=1}^{N_b}a_{j+N}^{(k)}\phi(x,y,z,x_j,y_j,z_j,d) \qquad (8)$$

$$\frac{\partial v^{(k)}}{\partial y}=\sum_{j=1}^{N}b_j^{(k)}\phi(x,y,z,x_j,y_j,z_j,c)+\sum_{j=1}^{N_b}b_{j+N}^{(k)}\phi(x,y,z,x_j,y_j,z_j,d) \qquad (9)$$

where

$$\phi(x,y,z,x_j,y_j,z_j,c)=\sqrt{(x-x_j)^2+(y-y_j)^2+(z-z_j)^2+c^2} \qquad (10)$$

The shape parameters c and d of the multiquadrics must not be equal so that basis functions in Eq. (8) and (9) are linearly independent. It will be shown that their values affect the accuracy of the solution. Insert Eqs. (8) and (9) into Eq. (4), and rearrange the result..

$$\frac{\partial w^{(k)}}{\partial z} = -\sum_{j=1}^{N} a_j^{(k)} \phi(x, y, z, x_j, y_j, z_j, c) - \sum_{j=1}^{N_b} a_{j+N}^{(k)} \phi(x, y, z, x_j, y_j, z_j, d)$$
$$-\sum_{j=1}^{N} b_j^{(k)} \phi(x, y, z, x_j, y_j, z_j, c) - \sum_{j=1}^{N_b} b_{j+N}^{(k)} \phi(x, y, z, x_j, y_j, z_j, d) \quad (11)$$

Approximation of the velocity components and other partial derivatives of the velocity components can be obtained since ϕ can be easily integrated and differentiated. For the purpose of iterative determination of $N + N_b$ unknown coefficients $a_j^{(k)}$ and $b_j^{(k)}$, nonlinear terms in Eqs. (5) and (6) are linearized by a scheme proposed by Ferziger and Peric [13]. For example,

$$u^{(k)} \frac{\partial^2 u^{(k)}}{\partial x \partial y} = u^{(k-1)} \frac{\partial^2 u^{(k)}}{\partial x \partial y} + u^{(k)} \frac{\partial^2 u^{(k-1)}}{\partial x \partial y} - u^{(k-1)} \frac{\partial^2 u^{(k-1)}}{\partial x \partial y} \quad (12)$$

After linearization, Eqs. (5) and (6) represent $2N$ equations for $(x, y, z) = (x_i, y_i, z_i)$ (i = 1, 2, ..., N). Boundary conditions for u, v and w yield $3N_b$ more equations. Therefore, the resulting system of equations can be solved by the method of least square because there are more equations than unknowns. Initially, let $a_j^{(0)} = b_j^{(0)} = 0$. The iteration process is continued until the following convergence criterion is satisfied:

$$\sqrt{\frac{1}{N_i} \sum_{i=N_b+1}^{N} \left(1 - \frac{f_i^{(k-1)}}{f_i^{(k)}}\right)^2} < 10^{-5} \quad (13)$$

where f represents a velocity component.

4 RESULTS AND DISCUSSION

The domain for the three-dimensional test problem is a $1 \times 1 \times 1$ cube. There are 512 test nodes located at $(\frac{i}{8} + \frac{1}{16}, \frac{j}{8} + \frac{1}{16}, \frac{k}{8} + \frac{1}{16})$ with integers i, j and k running from -4 to 3. There are 729 nodes uniformly distributed in the domain, forming a cube grid. Exact solution for this problem is

$$u_{exact}(x, y, z) = \nu + 2e^{(x+y+z)} \quad (14)$$
$$v_{exact}(x, y, z) = \nu - e^{(x+y+z)} \quad (15)$$
$$w_{exact}(x, y, z) = \nu - e^{(x+y+z)} \quad (16)$$

From this exact solution; boundary condition is generated, and numerical solution is determined by using the proposed method. In the following results, it is shown how ϵ_u, ϵ_v and ϵ_w vary with the shape parameters c and d.

The test problem having Dirichlet boundary condition is considered. Let $(\xi_i, \eta_i, \gamma_i)$ be coordinates of a test node. Velocity components at the test node can be calculated after coefficients have been determined. Subsequently, errors are computed from

$$\epsilon_f = \sqrt{\frac{\sum_{i=1}^{N_t} [f_{numer}(\xi_i, \eta_i, \gamma_i) - f_{exact}(\xi_i, \eta_i, \gamma_i)]^2}{\sum_{i=1}^{N_t} [f_{exact}(\xi_i, \eta_i, \gamma_i)]^2}} \quad (17)$$

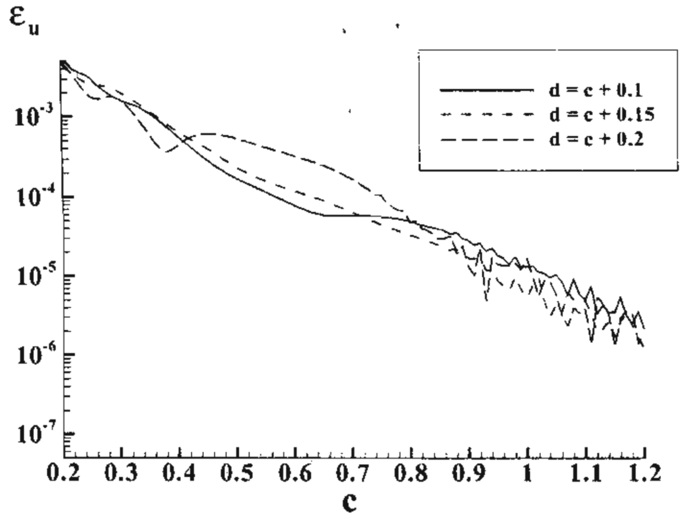

Figure 1: Variation of error of velocity component ϵ_u with the shape parameters c and d.

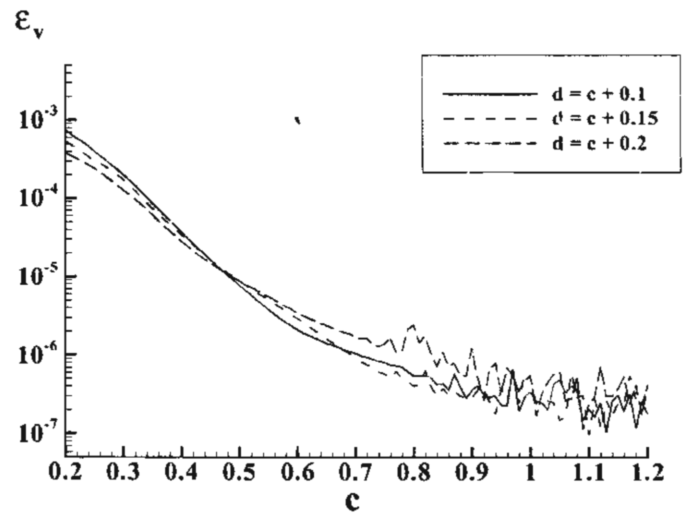

Figure 2: Variation of error of velocity component ϵ_v with the shape parameters c and d.

where N_t is the number of test nodes, and f represents velocity component u, v or w.

Figures 1, 2, and 3 show influences of the shape parameters c and d on ϵ_u, ϵ_v, and ϵ_w, respectively, for $\nu = 1$. Solution is more accurate as c is increased. When c is too large, however, it is found that no converged solution can be found. A large value of c is associated with high condition number of the coefficient matrix of the system of linear equations. Since the computing machine used in this study has a limited precision, an ill-conditioned system of linear equations cannot be solved with high precision. This may be a reason why the proposed method does not converge when a certain value of c is reached. In addition, Figs. 1, 2, and 3 also show that solutions are relatively insensitive to the shape parameter d between $c + 0.1$ and $c + 0.2$.

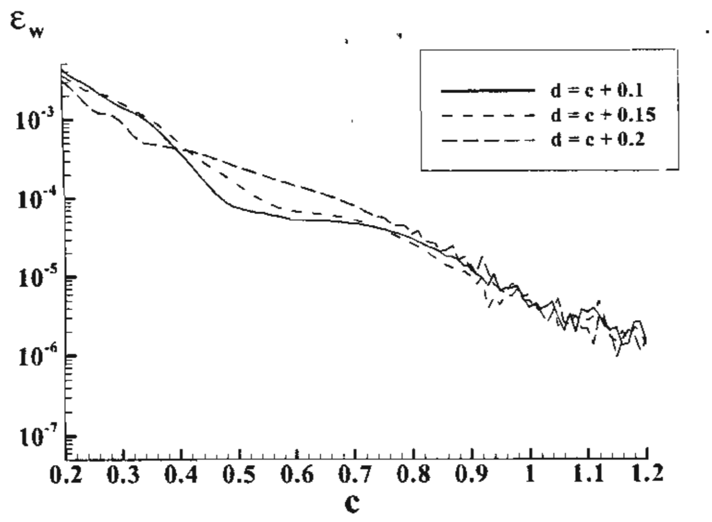

Figure 3: Variation of error of velocity component ϵ_w with the shape parameters c and d.

5 CONCLUSIONS

This paper presents an alternative approach for solving the three-dimenisional Navier-Stokes equations, in which pressure and one of the velocity components are eliminated, and the four governing equations are reduced to two higher-order partial differential equations of the remaining two velocity components. The resulting equations are solved by a meshless collocation method that uses multiquadrics and associated functions as basis functions. Inspection of the solution to a test problem by the proposed method reveals that shape parameters of multiquadrics influence the accuracy of the solution.

REFERENCES

[1] J. C. Tanhill, D. A. Anderson, and R. H. Pletcher, *Computational Fluid Mechanics and Heat Transfer* (2nd edn). Taylor and Francis, Washington DC, 1997.

[2] E. J. Kansa, Multiquadrics - A scattered data approximation scheme with applications to computational fluid-dynamics-II solutions to parabolic, hyperbolic and elliptic partial differential equations. *Computers and Mathematics with Applications*, **19**, 147-161, 1990.

[3] M. Zerroukat, H. Power, and C. S. Chen, A numerical method for heat transfer problems using collocation and radial basis functions. *International Journal for Numerical Methods in Engineering*, **42**, 1263-1278, 1998.

[4] Y. C. Hon and X. Z. Mao, An efficient numerical scheme for Burgers' equation. *Applied Mathematics and Computation*, **95**, 37-50, 1998.

[5] A. I. Fedoseyev, M. J. Friedman, and E. J. Kansa, Continuation for nonlinear elliptic partial differential equations discretized by the multiquadric method. *International Journal of Bifurcation and Chaos in Applied Sciences and Engineering*, **10**, 481-492, 2000.

[6] J. Li and C. S. Chen, Some observations on unsymmetric radial basis function collocation methods for convection-diffusion problems. *International Journal for Numerical Methods in Engineering*, **57**, 1085-1094, 2003.

[7] X. Zhoua X, Y. C. Hon, and K. F. Cheung, A grid-free, nonlinear shallow-water model with moving boundary *Engineering Analysis with Boundary Elements*, **28**, 967-973, 2004.

[8] D. L. Young, S. C. Jane, C. Y. Lin, C. L. Chiu, and K. C. Chen, Solutions of 2D and 3D Stokes laws using multiquadrics method. *Engineering Analysis with Boundary Elements*, **28**, 1233-1243, 2004.

[9] M. Mai-Duy and T. Tran-Cong, Numerical solution of Navier-Stokes equations using multiquadric radial basis function networks. *International Journal for Numerical Methods in Fluids*, **37**, 65-86, 2001.

[10] C. Shu, H. Ding, and K. S. Yeo, Computation of incompressible Navier-Stokes equations by local RBF-based differential quadrature method. *CMES - Computer Modeling in Engineering and Sciences*, **7**, 195-205, 2005.

[11] H. Ding, C. Shu, K. S. Yeo, and D. Xu, Numerical computation of three-dimensional incompressible viscous flows in the primitive variable form by local multiquadric differential quadrature method. *Computer Methods in Applied Mechanics and Engineering*, **195**(7-8):516-533, 2006

[12] S. Chantasiriwan, Cartesian grid methods using radial basis functions for solving Poisson, Helmholtz, and diffusion-convection equations. *Engineering Analysis with Boundary Elements*, **28**, 1417-1425, 2004.

[13] J. H. Ferziger and P. Milovan, *Computational Methods for Fluid Dynamics*. Springer, Berlin, 1997. 115.

SCIENCE DIRECT

INTRODUCTION

The **ScienceDirect TOP25 Hottest Articles** is a free quarterly service from ScienceDirect. When you subscribe to the **ScienceDirect TOP25**, you'll receive an e-mail every three months listing the ScienceDirect users' 25 most frequently downloaded journal articles, from any selected journal among more than 2,000 titles in the ScienceDirect database, or from any of 24 subject areas.

Now you can keep track of the latest trends in your speciality and find out what your colleagues are reading. A simple click on any of the listed articles will take you to the journal abstract, and of course, you have the option to download any article straight to your desktop, depending on your access rights.

Read more about how the TOP 25 is generated and what it reflects.

TOP 25 HOTTEST ARTICLES ON ScienceDirect

Check out the ScienceDirect TOP25 Hottest Articles within your are of interest.

Subject Area: Engineering

Journal: Engineering Analysis with Boundary Elements

Select your ScienceDirect TOP25 Hottest Articles list using the drop-down mer (above). Select "all subject areas" to produce a list of the most downloaded articles across ScienceDirect. Select any subject area and "all journals" to produce the TOP25 list across all journals in the chosen subject area. Select b a subject area and a journal to see the hottest articles from a particular journ Try our new archive function (below) to scroll through TOP25 lists from previo quarters.

TOP25 articles within the journal: Engineering Analysis with Boundary Element

BROWSE ARCHIVE TOP 25s

OCT - DEC 2004

1. Cartesian grid methods using radial basis functions for solving Poisson, Helmholtz, and diffusion-convection equations • Articl
Engineering Analysis with Boundary Elements, Volume 28, Issue 12, 1 December 2004, Pages 1417-1425
Chantasiriwan, S.
2. Accuracy and efficiency of higher-order boundary element meth for steady convective heat diffusion in three-dimensions • Artic
Engineering Analysis with Boundary Elements, Volume 28, Issue 12, 1 December 2004, Pages 1475-1491
Grigoriev, M.M.;Dargush, G.F.
3. Electrostatic BEM for MEMS with thin conducting plates and she Article
Engineering Analysis with Boundary Elements, Volume 28, Issue 12, 1 December 2004, Pages 1427-1435
Bao, Z.;Mukherjee, S.
4. Fundamental solutions for thick sandwich plates • Article
Engineering Analysis with Boundary Elements, Volume 28, Issue 12, 1 December 2004, Pages 1437-1444
Boykov, I.V.;Boykova, A.I.;Ventsel, E.S.
5. Stress analysis of an infinite anisotropic elastic medium contain inclusions using the boundary point method • Article
Engineering Analysis with Boundary Elements, Volume 28, Issue 11, 1 November 2004, Pages 1293-1302
Dong, C.Y.;Lee, K.Y.
6. Symmetric Galerkin boundary element computation of T-stress stress intensity factors for mixed-mode cracks by the interactio integral method • Article
Engineering Analysis with Boundary Elements, Volume 28, Issue 11, 1 November 2004, Pages 1335-1350
Sutradhar, A.;Paulino, G.H.
7. A boundary element method for the numerical investigation of near-wall fluid flow with vortex method simulation • Article
Engineering Analysis with Boundary Elements, Volume 28, Issue 11, 1 November 2004, Pages 1405-1416
Khatir, Z.